NETWORK MODELING OF DRUG RESISTANCE AND EFFICACY IN CANCER THERAPY

A Dissertation

by

RADHIKA SARAF

Submitted to the Office of Graduate and Professional Studies of
Texas A&M University
in partial fulfillment of the requirements for the degree of

DOCTOR OF PHILOSOPHY

Chair of Committee,	Aniruddha Datta
Committee Members,	Yang Shen
	P.R. Kumar
	Raktim Bhattacharya
Head of Department,	M. Begovic

May 2020

Major Subject: Electrical Engineering

ABSTRACT

The research outlined in this proposal has three objectives: (i) to model biological pathways involved in cancer using data and prior knowledge; (ii) to investigate the mechanism of action for drugs that are used in cancer therapy; and (iii) to predict the efficacies of drug combinations for effective cancer therapy.

Several of the chemotherapeutic drugs available in the market today target the genes belonging to the cell proliferation or cell survival pathways. However, cancer cells manage to evade death despite being treated by these drugs. The ability of cancer cells to resist chemotherapy is called drug resistance or chemoresistance. Design of cancer therapy involves identifying potential key intervention points in the cell signaling pathways and looking for drug cocktails that could be effective in controlling these points. By targeting the molecules that sensitize cancer cells to cell death, we can devise a strategy to overcome drug resistance.

We employ mathematical modeling and simulation to first, demonstrate how drug resistance occurs in cancer cells and second, which drugs or combinations of drugs can sensitize the cells and achieve robust cell killing.

We modeled the biological pathways instrumental in metastatic melanoma, osteosarcoma and glioblastoma as Boolean networks. STAT3, a signal transducer and activator of transcription factor was identified as an important intervention point in cancer cell signaling pathways. We were able to verify that the inhibition of STAT3 is crucial in order to increase sensitivity of the melanoma and osteosarcoma cells to cell death. The Chinese herbal drug, Cryptotanshinone was chosen since it is known to be an effective STAT3 inhibitor. We predicted the efficacies of different drug combinations used in the treatment of the three cancers.

DEDICATION

To my mother.

To the greater good and the values I was raised with.

To the Aggie Spirit.

ACKNOWLEDGMENTS

CONTRIBUTORS AND FUNDING SOURCES

Contributors

Funding Sources

NOMENCLATURE

CT	Cryptotanshinone
DR5	Death Receptor 5
GBM	Glioblastoma Multiforme
GDSC	Genomics of Drug Sensitivity in Cancer
OS	Osteosarcoma
STAT3	Signal Transducer and Activator of Transcription 3
TMZ	Temozolomide
TRAIL	Tumor Necrosis Factor Related Apoptosis Inducing Ligand

TABLE OF CONTENTS

Page

LIST OF FIGURES

LIST OF TABLES

1. INTRODUCTION

1.1 Background

1.1.1 Introduction to Molecular Biology and Cancer

Genetic information is passed from a cell to its daughter cells at the time of cell division. This genetic information is stored in deoxyribonucleic acid (DNA) molecules in the nucleus of the cell. Genes are short stretches of DNA, that are responsible for the synthesis of proteins [2].

Genes rely on ribonucleic acid (RNA) molecules to carry out protein synthesis. The central dogma of molecular biology is the principle that states that the flow of genetic information in a cell is from DNA to RNA to protein. The process of copying the DNA into the strands of RNA is called transcription. When a gene is being transcribed, it is said to be expressed. A cell can vary its gene expression in proportion to the need for a particular protein [2].

The signaling networks of genes in the body govern the biological processes in cells. The receptors in the surface of a cell are responsible to detect signals from sources external to the cell. Whenever an external stimulus is incident on the cell, it reacts with an appropriate response. The responses of the cell are governed by the genes in the signal-transduction cascade.

Genes can give commands to cells and control cell fate. Cell death or apoptosis can be induced by a loss of survival signals to a cell. Cell proliferation is initiated by the binding of growth factors to the trans-membrane receptors. The balance between controlled cell proliferation and cell death is termed as cell cycle control [2].

Abnormalities in cell cycle control are a characteristic of cancer, and this is accompanied by uncontrolled growth or tumors [3]. The disruption in normal function of the cells could be due to aberrant signaling among the genes. This genetic instability in tumors could be attributed to genetic alterations and could lead to further genetic mutation [4].

Our goal is to produce a model that captures the abnormalities in cell cycle control. We investigate how gene expression is affected by mutant genes and whether that can explain how genetic

instability progresses in cancer cells.

1.1.2 Genetic Regulatory Networks

The signal-transduction cascade in the cells which leads to activation or inhibition of genes can be modeled as a pathway [2]. Cellular signaling pathways represent the causal interconnection between the genes. A causal relationship implies that a change in the expression of one gene affects the other. Biological experiments and assays are able to discover direct interactions between genes. In this manner, many of the cellular signaling pathways have been established [5, 6, 7].

Genetic regulatory networks capture the multivariate interactions between genes. Mathematical modeling is a tool that is employed by researchers to discover new or possibly hidden gene interactions. Modeling techniques including but not limited to differential equations, Bayesian networks and both deterministic and probabilistic Boolean networks [8, 9, 10] have been used to study genetic regulatory networks.

We choose to model the biological pathways in cancer using deterministic Boolean networks. Boolean networks are formalized using current biological knowledge from the literature.

1.1.3 Selection of Intervention Points

In cancer cells, genes responsible for cell growth are usually overexpressed whereas tumor suppressor genes are inactive. The deviation from normal gene expression in cancer cells can be attributed to genetic mutation. Mutant genes can also cause overexpression or irregular inhibition of their downstream targets.

The irregularites of gene expression can be modeled in the genetic regulatory network as faults. A fault can occur when a node is stuck at a particular state. A stuck node is one that does not respond to upstream signaling; it stays in its current output state irrespective of the inputs it receives. The identification of faults in a network allows us to design a cancer therapy to correct these faults [3].

Mutations in the cell proliferation or cell survival pathways are frequently found in many cancers [11, 12, 1]. Conventional cancer therapies use drugs that target cell proliferation or cell sur-

vival pathways, however the cancer cells treated with these drugs manage to evade cell death. This property of cancer cells is known as chemoresistance or drug resistance.

It is noteworthy that in both normal and cancer cells, the expression of pro-apoptotic factors can be detected [13]. This indicates that the upstream defects in cancer most likely inhibit apoptosis by an increase in the activity of anti-apoptotic genes. This fact is useful when trying to understand drug resistance. A possible mechanism for drug resistance is the failure to induce apoptosis in cancer cells. Typically, most cancer cells deactivate the pathways to cell death and simultaneously heighten the activities of the cell proliferation and growth pathways.

In order to design an effective cancer therapy, we must look at a combination of drugs that counters all the effects of cancer cells. Drug cocktails should activate cell death pathways while concomitantly inhibiting cell survival pathways. Combination therapy can curb cell proliferation, sensitize cells to apoptosis and thus, ensure robust cell death [3].

We model the cell signaling pathways responsible for drug resistance in cancer cells . Our secondary goal is to predict the efficacies of drugs and drug combinations that can potentially induce apoptosis in a robust fashion.

1.2 Research Design and Methods

1.2.1 Current State of Drug Discovery

Drug discovery requires the application of different conceptual and analytical approaches to biological processes. The development of a new drug involves identifying new targets, validating said targets, biological synthesis of drugs, considering the pharmacokinetics, studying the potential side effects of the drug, testing and clinical trials. This process incurs high costs and does not promise great success rates [14]. Recent research shows that even non-cancer drugs can be repurposed to treat cancer, this can offset costs and expand the therapeutic options. The functional testing of all candidate genetic targets or candidate drug combinations becomes infeasible as the number of candidates increases [15].

Molecular and cell biologists are responsible for identifying and evaluating potential targets in the early stages of drug development. The traditional method of ranking drug targets depends on extensive literature survey of current research and treatment and the knowledge of the researcher. The mental integration of data from a variety of sources can prove to be challenging and is vulnerable to human error. Once a potential target is identified, it needs to be validated through biological experimentation. This trial-and-error method can prove to expensive in terms of resources and time; limitations in the budget and accessibility to appropriate testing facilities can also prove to be obstacles [16].

On the other hand, the newer methods of prioritization of drug targets require access to ample amounts of data and are computationally expensive. High throughput data techniques usually produce only one type of "-omic' data (genomic, proteomic, metabolomic). Data-based modeling using such data requires specific or proprietary data processing and analysis platforms. The correlative nature of this data makes it difficult to study the exact causal relationships between different data points. Many genes or proteins can have dual roles in biological processes such as the overexpression of STAT3 in several cancer cells. It might not be possible to determine through such "-omic" approaches whether STAT3 upregulation is the cause or effect of cancer progression

[16, 17, 18]. Moreover, the results of the computational models are not easy to interpret and can even conflict with other large-scale ranking techniques. A major drawback of such approaches is low experimental reproducibility, which means that the ranking is subject to change each time the algorithm is run [15].

We can take a closer look at the latest computational models that predict the drug target ranking. Project Score [19] seems to be a promising prioritization technique, it uses a cellular fitness score to rank targets and the data is collected using Crispr/Cas9 screens. The potential demerit of Project Score is that it is not tailored to a specific cancer and it fails to represent all the cell line mutations found in GBM. DrugComb [15] is a web-based portal that performs large-scale integration of cancer drug screen data for different cell lines, however DrugComb deals with the drugs as a whole and doesn't provide information of how individual genetic targets in the GBM pathways could be ranked. The Genomics of Drug Sensitivity in Cancer (GDSC) [20] database provides information about drug sensitivity for different cell lines as well as molecular markers of drug response. The GDSC database considers only anti-cancer drugs, however while designing optimal cancer therapies, it makes sense to include the targets of non-cancer drugs [14].

Boolean network modeling offers a tradeoff between data-based modeling and the traditional biological methods. Boolean networks are deterministic models that are based on established biological knowledge, and can be used to ease the computational burden of the researcher. They are representative of the current state of information that is available about the pathways in cancer, and can be updated with ease to reflect the latest research. Unlike data-based techniques, regenerating the ranking after modification does not require huge computational power. Our modeling technique seeks to bridge the gap between designing computational models and understanding biological complexities of cancer. We include existing genetic information as well as research about chemotherapeutic, herbal and non-cancer drugs. We seek to propose an optimal and robust strategy to combat cancer.

1.2.2 Boolean Network Modeling

The development of chemoresistance in cancer cells involves various biological pathways. The key lies in integrating the pathways and modeling the cross talk between them. The components of these pathways are represented as a Boolean network with multiple inputs and multiple outputs. The possible mutations in genes that can lead to cancer are captured by faults in a combinatorial circuit and the model is used to theoretically predict the effectiveness of a drug for inducing apoptosis in cancer cell lines.

In the paradigm of Boolean network modeling, each gene is a node and its direct interaction with another gene is represented as an edge. Gene expression is binarily quantized: a gene, if expressed is considered to be ON (State 1) and if not expressed, is considered to be OFF (State 0). If two or more genes interact to activate or inhibit a third gene, such relationships are modelled with the use of logic gates. The genetic regulatory network can then be thought of as a multi-input multi-output (MIMO) digital logic circuit.

A cancerous cell will not have the same input-output mapping as a normal one. This is due to the anomalies that occur in the biological pathways of cancer cells. Malfunctioning genes lead to uncontrolled cell proliferation, increased inflammation and failure of the apoptotic pathways. These irregularities of tumor cells can be thought of as faults in the Boolean network, particularly stuck-at faults. A stuck-at fault occurs when a node in the network is permanently set to a fixed value of either zero (stuck-at-0 fault) or one (stuck-at-1 fault) [3]. This implies that the circuit will not change as expected when subjected to a certain set of inputs. The output vector of a faulty network then will be independent of the other signal values in the regulatory circuit. An over-expressed gene can be denoted as a stuck-at-1 fault. This notion is common in cancer where oncogenes tend to display similar faulty behaviour, irrespective of what input they receive and evade any corrective action from upstream. The effect of such a fault can be corrected by using a drug as shown in Figure 1.1. On the other hand, a stuck-at-0 fault can result when a gene becomes permanently inactive, independent of the activity status of its upstream regulators. For example, a mutated p53 gene in a cancer cell will remain inactive despite being phosphorylated as a result of

6
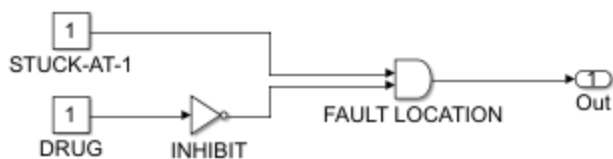
Figure 1.1: Boolean representation of the drug action countering a stuck-at-one fault
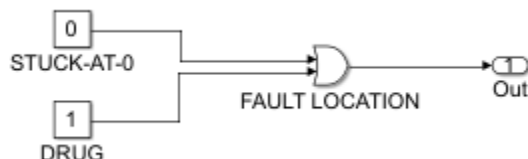
Figure 1.2: Boolean representation of the drug action countering a stuck-at-zero fault

cellular DNA damage. This situation, common to several cancers, is one where a drug can correct a stuck-at-0 fault as shown in Figure 1.2.

1.2.3 Key Intervention Points

Commonly known mutations can be modeled as faults. Nodes that are downstream of mutant genes are considered as reporter nodes. The expression of reporter nodes can be measured to quantify the effect of the mutated nodes upstream. The faults and the corresponding reporter nodes could help us identify the key intervention points for cancer therapy. We seek to map the states of reporter nodes as outputs corresponding to the mutated nodes as inputs.

Biological pathway information indicates that STAT3, a signal transducer and activator of transcription plays a crucial role in cancer cell signaling [21, 22, 23, 24, 25, 26, 27, 28, 29]. We examine the role that STAT3 plays in the progression of genetic instability in cancer cells. We test whether inhibition of STAT3 produces cell death in cancerous cells.

1.2.4 Drug Intervention

Drugs used to treat cancers try to restore the normal cell cycle function through action on the cell signaling pathways; they are used to counter the action of mutant genes. Drugs are considered

as inputs, and their effects can be estimated by observing the expression of the corresponding output nodes downstream.

A drug can either activate or inhibit a certain target gene. Some drugs are known to have more than one target gene. In combination therapy, we can use drugs of all kinds and in different proportions. The goal is usually to find the optimal combination of drugs that achieve cell death in a robust manner.

Cryptotanshinone (CT), a Chinese herbal derivate is one of the drugs that has been shown to restore sensitivity to cell death [30]. STAT3 is a known target of CT in various cancers [31, 32]. We study the action of CT on the various biological pathways and predict its efficacy in combination with other drugs.

Temozolomide (TMZ) is a drug that enhances the effect of radiotherapeutic intervention in cancer cells. The resistance to TMZ can be attributed to the DNA repair pathway [33, 34]. We investigate the pathways that could contribute to the resistance to TMZ, and predict drug combinations that could robustly kill cancer cells despite such resistance.

1.2.5 Cancer Immunotherapy and its Relationship to the Proposed Research

Chemoresistance is linked with TRAIL resistance in certain cancers [35]. TNF-related apoptosis-inducing ligand (TRAIL) is implicated in immunosurveillance, which is the ability of the immune system to recognize pathogens and activate the mechanisms to neutralize their effect [36]. TRAIL is a component of the extrinsic apoptotic pathway, and is responsible for causing cell death in response to appropriate stimuli.

The human body reacts to threats by relying on its immune system and by proper functioning of the cellular signaling pathways. Recent immunotherapy research involves exploiting the body's immune system to fight against cancer. Decreasing TRAIL resistance is one of the methods employed in immunotherapy. TRAIL resistance is also associated with the mutations in cell survival pathways [13, 35]. Treatment strategies that involve sensitization of the cancer cells to extrinsic apoptosis have shown promise [37].

We model TRAIL resistance and its effect on chemoresistance in cancer cells. A drug that can

8

overcome both types of resistance will be truly effective. We estimate the efficacies of drugs that target the pathways responsible for chemoresistance and TRAIL resistance. The model will help us to come up with drug combinations that aid immunotherapeutic approaches to cancer treatment.

1.2.6 Prioritization of Genetic Targets

Protein or mRNA modulation techniques are employed during target validation, where the target is altered by an external agent and the change in the cellular viability is measured [17]. Cellular viability is the measure of live, healthy cells in the population of cells under experiment, and is inversely proportional to the efficacy of the genetic target.

As an alternative to protein or RNA modulation, we simulate the modulation of the genetic target and measure the change in the output metric. Assume that Boolean circuit has N nodes numbered from 1 to N. In each run of the simulation, we force a particular node in the circuit to one, which is equivalent to inducing expression of the corresponding gene, and we measure the change in the output. We will perform N runs with node $i = \{True \ \forall \ i \in [1, N]\}$. Similarly, we follow the same steps by forcing every node to zero, and measuring the effect of inhibition of one gene at a time. We will perform N runs with node $i = \{False \ \forall \ i \in [1, N]\}$. As a result, we have a list of $2N$ measurements of the output metric each corresponding to a particular Boolean combination in the network. Sorting the list on the basis of the output metric gives us the key intervention points. The most potent intervention point has the maximum effect on the output metric. This is useful while developing single-target therapies.

This technique can be extended to measure the effect of modulating more than one target at a time. We can simulate the effect of altering combinations of targets by forcing groups of nodes to a set of logical values in every run. This is useful while develop multiple-target therapies.

We simulate protein and mRNA modulation of various genetic targets involved in cancer progression to isolate the best possible drug combination for treatment of that cancer.

2. MELANOMA[1]

2.1 Current State of Cancer Therapy for Melanoma

Melanoma is one of the most prevalent and aggressive forms of skin cancer. Metastatic melanoma cells are known to develop resistance to most of the commonly used drugs and therapy [38]. TRAIL-induced apoptosis is a desirable method to treat melanoma since, unlike other treatments, it does not harm non-cancerous cells.

TRAIL resistance is associated with the mutations in cell survival pathways and the pro-inflammatory nFκB pathway [13, 35, 39]. Another possible reason for the development of TRAIL resistance is due to the lower expression of death receptors - death receptor 4 (DR4) and 5 (DR5) in the extrinsic apoptosis pathway [35].

2.1.1 Key Intervention Points in Melanoma

STAT3 plays a part in decreasing TRAIL cytotoxicity in metastatic melanoma cells [23]. It is a major influence on the various pathways involved in developing TRAIL resistance, which makes STAT3 a good candidate to induce TRAIL sensitivity [28, 29]. The STAT3 pathway is shown in Figure 2.1.

2.1.2 Drug Intervention in Melanoma

There are several existing drugs that act at different points in the cell survival and proliferation pathways as is shown in Figure 2.2; however none of them have been proven significantly effective against melanoma [38].

Cryptotanshinone (CT) is a herbal compound derived from the roots of the plant Salvia milti-orrhiza Bunge. CT can restore TRAIL sensitivity and induce apoptosis in A375 melanoma cells, by increasing DR5 expression via the induction of CHOP (CCAAT/enhancer-binding protein-homologous protein) [30]. In addition, STAT3 plays a key role in and is upstream of many of

---

[1]Parts of this chapter are adapted with permission from R. S. Saraf, A. Datta, C. Sima, J. Hua, R. Lopes, and M. Bittner, "An in-silico study examining the induction of apoptosis by cryptotanshinone in metastatic melanoma cell lines,"BMC Cancer, vol. 18, no. 1, p. 855, 2018
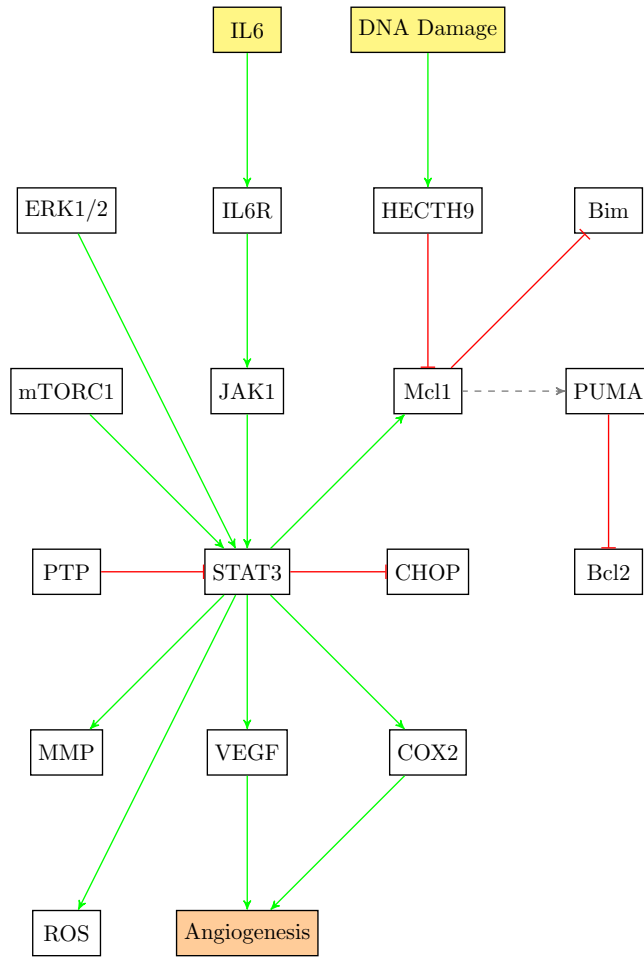
Figure 2.1: STAT3 pathway. Reprinted from Saraf 2018 ([1]).
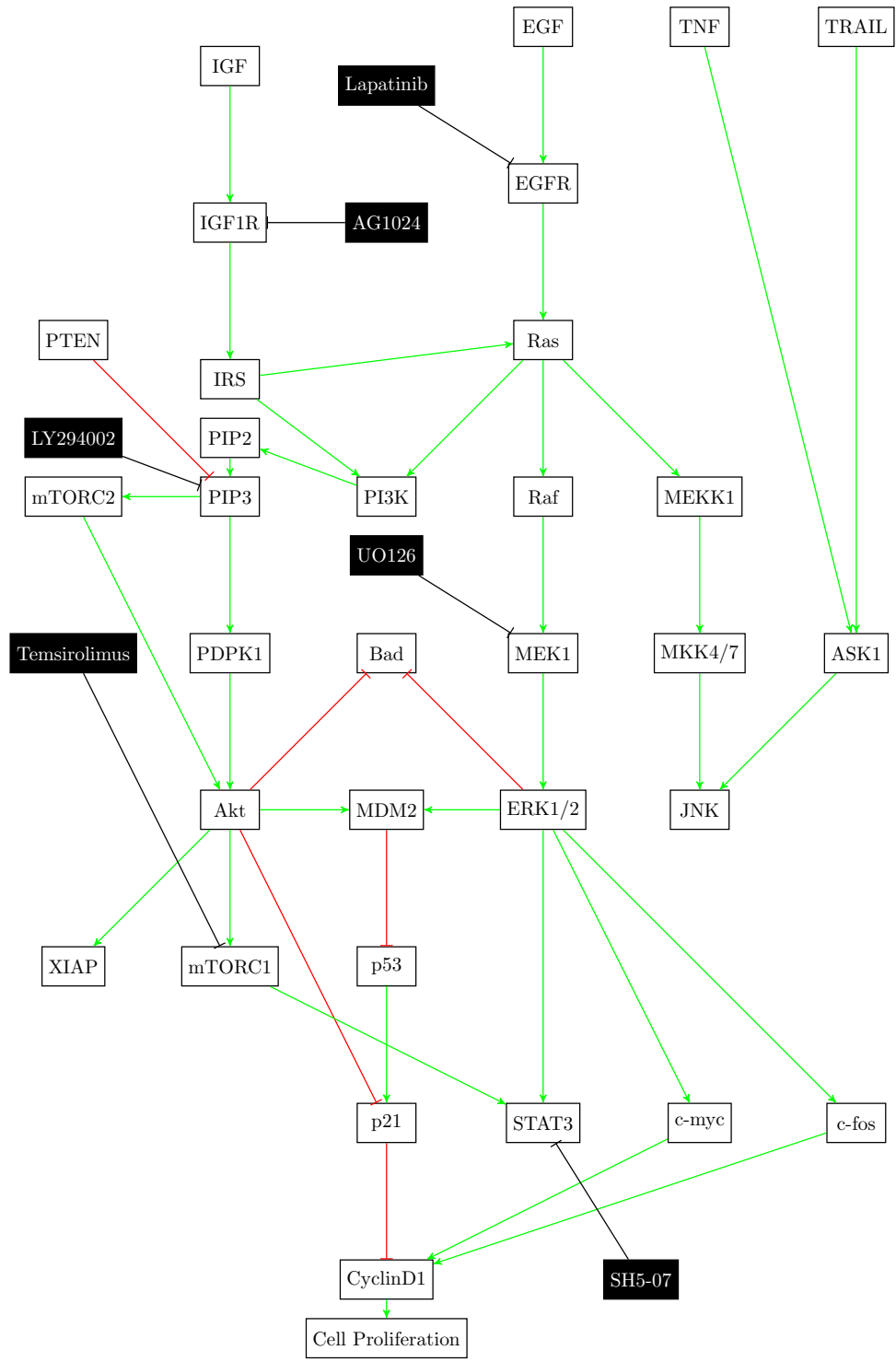
Figure 2.2: JNK, p53, PI3K/AKT/mTOR and MAPK/ERK pathways. Reprinted from Saraf 2018 ([1]).
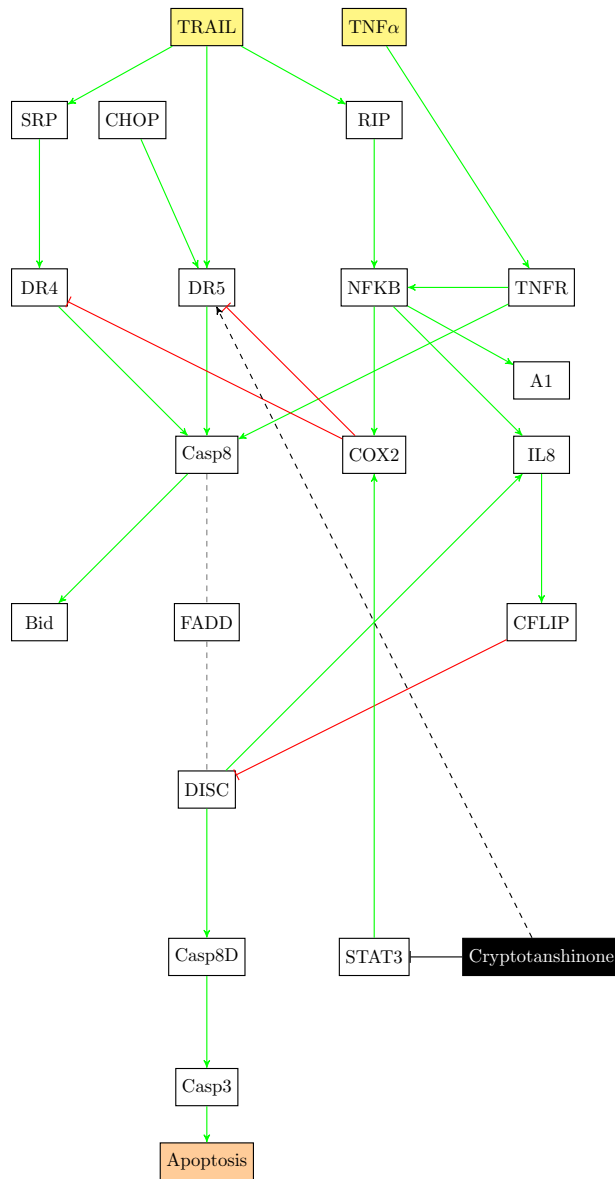
Figure 2.3: Extrinsic apoptosis and the nFκB pathways. Reprinted from Saraf 2018 ([1]).

the functions that CT affects and is a known target of CT in other cancers [31, 32]. The action of CT on the extrinsic apoptosis pathway can be seen in Figure 2.3.

2.2 Theoretical Network Modeling and Experimental Results for Melanoma

The various gene interactions in melanoma can be represented by biological pathways, which are all well documented [5, 6, 7]. Some of the interconnections derived during modelling these pathways are based on the interpretation of different research papers [40, 41, 42, 43, 44, 13, 45, 21, 46, 47, 48, 49, 50] by the author of this work. A subset of all possible interconnections and signaling pathways in the cell is considered, since the cancer of interest to us here is melanoma.

2.2.1 Results and Discusions

The static Boolean network considered here is used to represent a TRAIL resistant network and also includes information about how drug intervention could allow us to sensitize the melanoma cell lines to TRAIL. We focus on the TRAIL apoptotic pathway and on the effect the genes in the other pathways have on extrinsic cell death. The other inputs are DNA damage, ER stress and the growth factors that activate the pathways involved in melanoma. The outputs are all apoptotic factors, both pro- and anti- apoptotic, the ratio of which will decide whether the cell undergoes death. The input and output vectors are given by Equations 2.1 and 2.2 below:

$$\text{Input} = [\text{ER Stress, TNF}\alpha\text{, TRAIL, PTP, IL6, DNA Damage, IGF, EGF}] \tag{2.1}$$

$$\text{Output} = [\text{Casp8, Bid, Bad, Bim, Bak/Bax, Casp12, Bcl-XL, Bcl2, XIAP, Mcl1}] \tag{2.2}$$

For A375 melanoma cells, we consider 6 possible faults in our model. These correspond to the common mutations in the involved pathways and especially those that have been shown to cause TRAIL resistance [12]. All possible combinations of the faults have been simulated, that is 64 different configurations of the fault vector are considered. It is important to note that each component of the fault vector is either zero or one based on whether a particular fault is present or not. A one in the fault vector can denote a stuck-at-one fault or a stuck-at-zero fault, whichever is consequential for that particular gene. For instance, if the fault vector is $\begin{bmatrix} 1 & 0 & 0 & 0 & 0 & 0 \end{bmatrix}$, this implies that the Ras gene is faulty. Since it is a stuck-at-one type of fault, it means that Ras

14

is being constitutively expressed. On the other hand, presence of a stuck-at-zero fault represents the downregulation of the gene. For instance, when the fault vector equals $\begin{bmatrix} 0 & 0 & 1 & 0 & 0 & 0 \end{bmatrix}$, it means that PTEN is faulty and its suppressing action has failed. The fault vector components are given by Equation 2.3 and the types of faults are as listed in Table 2.1.

$$\text{Fault} = [\text{Ras, Raf, PTEN, p53, STAT3, DR5}] \tag{2.3}$$

Table 2.1: Genetic mutations in Melanoma represented as faults in the Boolean circuit. Reprinted from Saraf 2018 ([1]).

Stuck at 1	Stuck at 0
Ras	PTEN
Raf	p53
STAT3	DR5

The activity points of the different drugs on the pathways have already been shown in Figures 2.2 and 2.3. The components of the drug vector are displayed in Equation 2.4.

$$\text{Drugs} = [\text{CT, LY294002, Temsirolimus, UO126, Lapatinib, SH5-07, AG1024}] \tag{2.4}$$

Each component of the drug vector corresponds to whether or not that drug is applied, so a zero in the ith column indicates that the ith drug is not applied and vice versa. Since a major goal of this paper is to evaluate the action of Cyrptotanshinone, either by itself, or for enhancing the activity of other drug combinations, the combination of drugs considered here is limited to Cryptotanshinone alone and Cryptotanshinone in combination with the other drugs. Since there are six other drugs in the vector, a total of 2^6 drug combinations were tested. For instance, the drug vector $\begin{bmatrix} 1 & 0 & 0 & 0 & 0 & 0 & 0 \end{bmatrix}$ indicates that only Cryptotanshinone is applied.

For clarity of exposition, the entire Boolean network will be split up into three different components. Each component will follow the colour scheme shown in Figure 2.4 and the interconnections
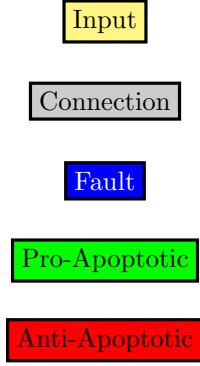
Figure 2.4: Legend showing the color coding scheme used in Figures 2.5, 2.6 and 2.7. Reprinted from Saraf 2018 ([1]).

between the three component networks will be indicated by the gray blocks. The three components are shown in Figures 2.5, 2.6 and 2.7. Figure 2.5 shows the relationship between the DNA damage input and how the apoptotic factors are affected upon the incidence of DNA damage, and this figure also helps in closely studying the effect of a p53 fault. Similarly, Figures 2.6 and 2.7 represent the gene interactions in the major pathways involved in melanoma.

2.2.2 Theoretical Simulation Results

We ran several rounds of simulations to test how Cryptotanshinone acts in combinations with the other drugs. To check the effectiveness of CT in increasing TRAIL cytotoxicity, we monitor its influence on the apoptosis induced. We are testing a TRAIL resistant static Boolean network. Here, it should be pointed out that a network can display trail resistance even in the absence of TRAIL, the resistance in that case having been residually left over from an earlier TRAIL induction event. The metric used to calculate the degree of apoptosis is:

$$\text{Apoptosis Ratio} = \frac{\sum \text{Pro-Apoptotic factors}}{\sum \text{Anti-Apoptotic factors}}$$

The apoptosis ratio is a measure of the relative change in apoptosis upon a change in conditions. The apoptosis ratio will change depending on different factors such as the values of the inputs, the presence of certain faults or the application of a drug. Changing the input combination to the
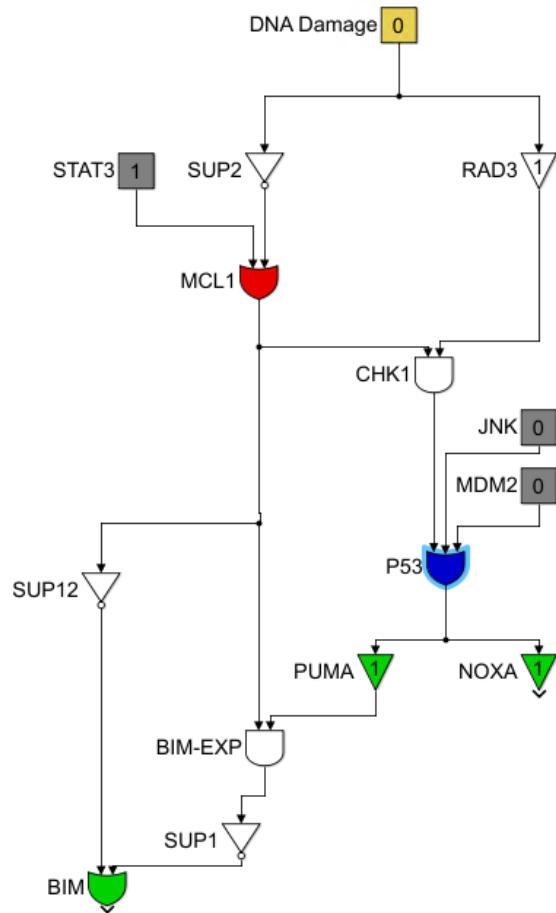
Figure 2.5: Boolean network for the DNA damage pathway. Reprinted from Saraf 2018 ([1]).
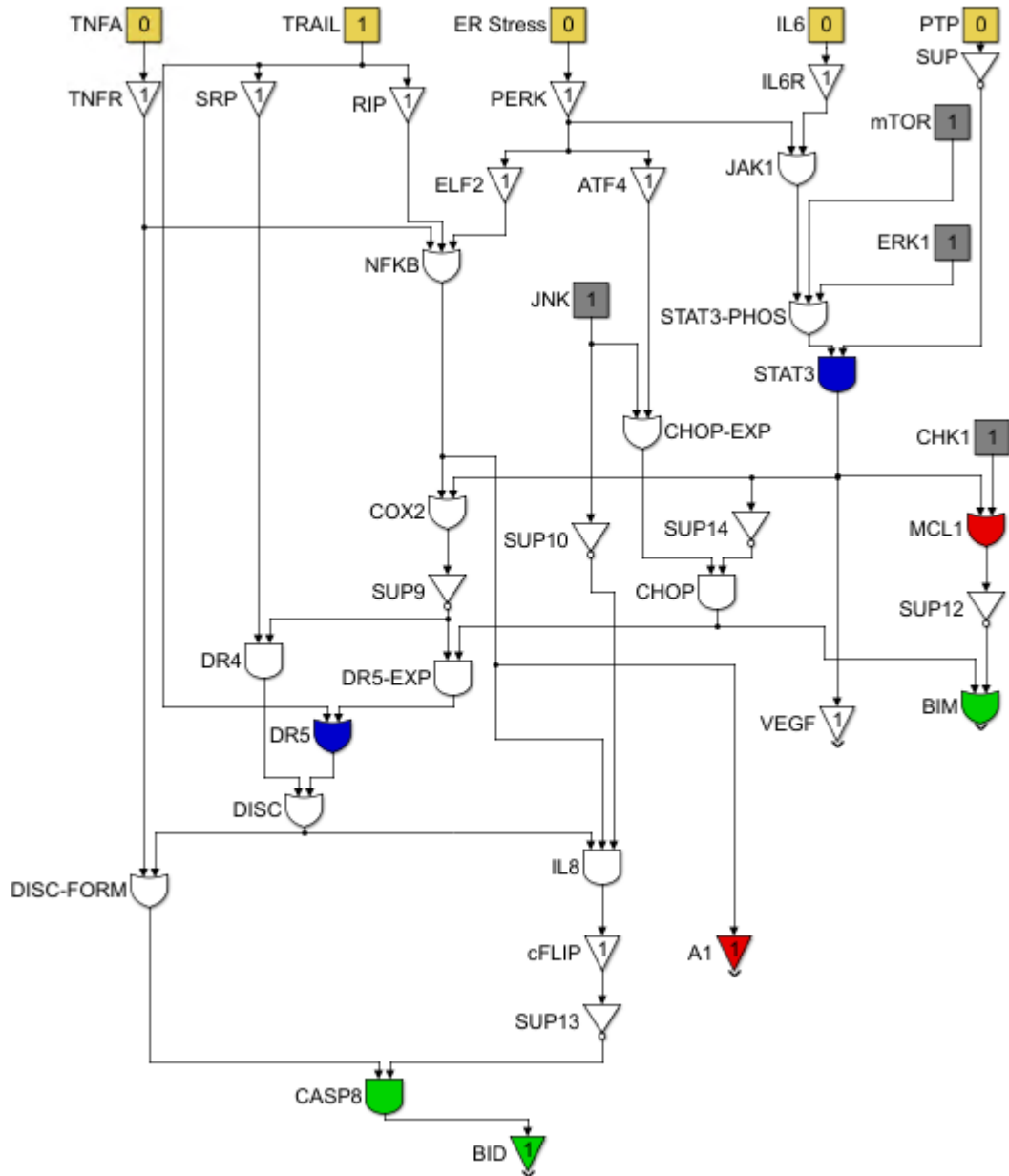
Figure 2.6: Boolean network for the TRAIL, ER Stress and STAT3 pathway. Reprinted from Saraf 2018 ([1]).
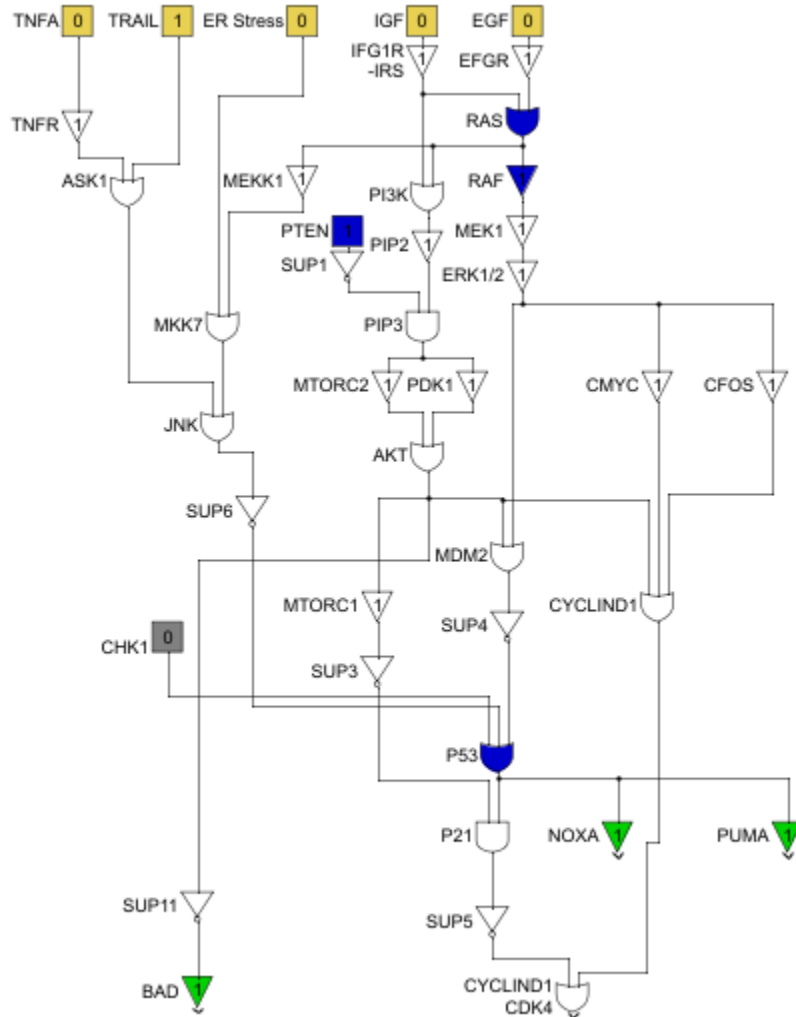
Figure 2.7: Boolean network for the PI3K/AKT/mTOR and MAPK/ERK pathway. Reprinted from Saraf 2018 ([1]).

Boolean network will change the value of the apoptosis ratio.

Simulation 1 : Apoptosis ratios for different inputs

Figure 2.8 presents three different states of the Boolean network, when the input vectors are :

1. '0000000' : 'No Input' which means that no growth factors, cytokines or stress signals are present.

2. '0010000' : 'TRAIL-induced apoptosis' which means that the TRAIL apoptotic pathway is active.

3. '1000000' : 'ER Stress induced Apoptosis' which considers ER Stress as the only active input.

Each color in the figure represents a different fault and drug combination. Blue stands for the situation where there is no fault and no drug; orange means that the DR5 and STAT3 faults are present; yellow shows the apoptosis induced by SH5-07 in the presence of these faults; and violet shows the apoptosis induced by CT in the presence of the two faults.

From Figure 2.8, we can see that the apoptosis ratio is 1.67 when there is 'No Input' and 'No Fault'. Moreover, we observe that CT is inducing apoptosis even in the absence of TRAIL or other apoptosis-inducing factors. This means that CT must be down-regulating the anti-apoptotic factors through its action on STAT3, thus leading to a relatively greater value of the apoptosis ratio.

A similar situation can be seen for the 'ER Stress induced apoptosis' case, where the apoptosis value increases upon application of CT. However, only its effect on STAT3 is not enough to explain the increased TRAIL sensitivity. This is clear by looking at the action of the other STAT3 inhibitor SH5-07, which is unsuccessful in inducing further apoptosis in the presence of the faults. Here, it is evident that the upregulation of DR5 by CT plays a role in increasing the apoptosis ratio.

Looking at the 'TRAIL-induced apoptosis' condition in the absence of a fault, we observe that the apoptosis ratio is large. DR5 and STAT3 faults reduce the value to almost half. The STAT3 inhibitor SH5-07 is unable to counter these faults. Cryptotanshinone though not able to regain the
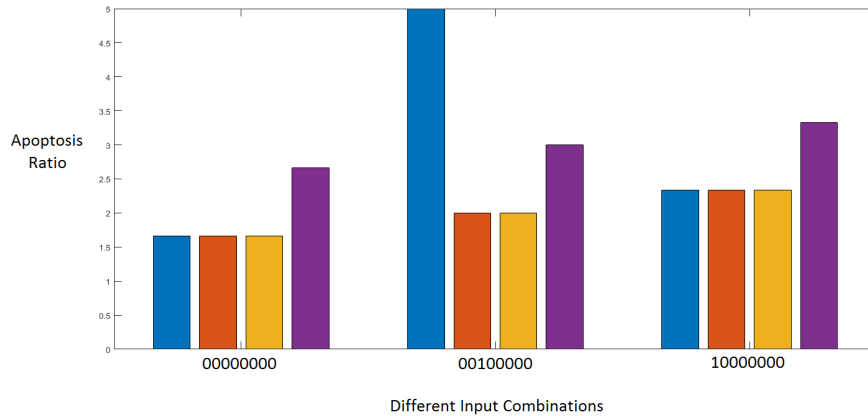
Figure 2.8: Apoptosis ratios for when different inputs are fed into the Melanoma Boolean network. Reprinted from Saraf 2018 ([1]).

fault-free value of apoptosis, is effective in increasing apoptosis despite the presence of faults. This seems to imply that the upregulation of DR5 is instrumental to restoring TRAIL sensitivity.

Simulation 2 : In the presence of simultaneous occurrence of all faults

The next simulation was run to test which single drug is the most effective in combination with CT. We considered the input to be TRAIL so that the input vector is '0010000' and assumed that all 6 faults are simultaneously present. The results are shown in Figure 2.9. The effect of LY294002, a PI3K inhibitor in combination with Cryptotanshinone seems to be better than the other combinations considered. The role of the cell survival pathway in TRAIL resistance is confirmed by the increase in TRAIL cytotoxicity via inhibition of PI3K, which is a major intervention point in the pathway.

Simulation 3 : All possible combinations of faults and drugs

The final simulation evaluates all fault combinations with all the drug combinations with and without Cryptotanshinone in Figures 2.10 and 2.11 respectively, when only the TRAIL input is active. Each row corresponds to a different drug combination (indicated by the corresponding drug vector) while each column corresponds to a different fault combination (indicated by the corresponding fault vector). The apoptosis value in each cell in the figure, thus, is the action that
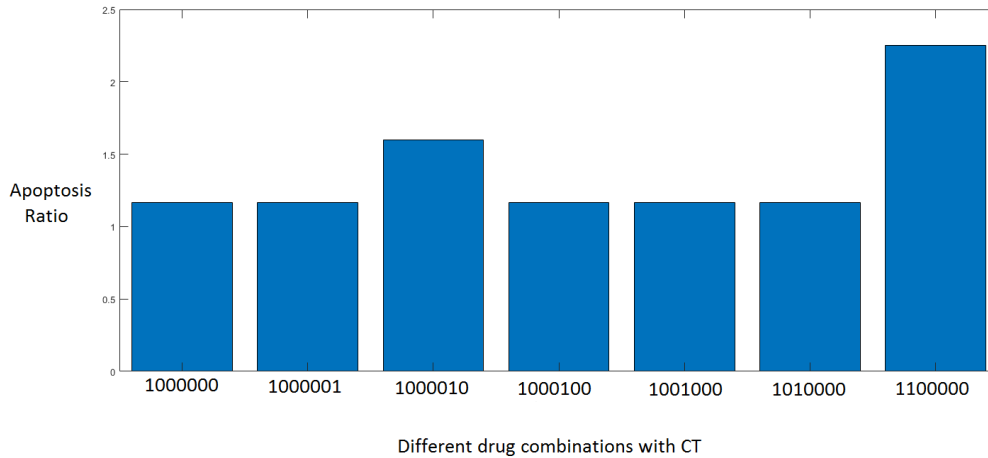
Figure 2.9: Apoptosis by CT in combination with a single drug in the presence of simultaneous occurrence of all faults. Reprinted from Saraf 2018 ([1]).

a drug vector has on that particular fault vector. Both the figures follow the same color scale. The red areas show regions of low apoptosis (apoptosis ratio=0.67) while the green areas show regions of maximum apoptosis (apoptosis ratio=5). A visual inspection shows that CT is successful in increasing TRAIL cytotoxicity for most combinations of faults. It is our conjecture in this paper that the effect of Cryptotanshinone on TRAIL resistance is through its action on STAT3 and DR5. The simulations seem to support this as they show that even in the presence of faults in other cell signaling pathways, such as p53, CT can solely through its action on STAT3 and DR5 diminish TRAIL resistance. Figure 2.10 does not have a single red cell, which means that CT is more effective in inducing apoptosis than any other drug combination considered in this paper. In contrast, Figure 2.11 has fewer green cells, which seems to point towards Temsirolimus, an mTORC1 inhibitor [48] to perform better than the other drugs in the absence of Cryptotanshinone. LY294002 in combination with CT seems to be the most effective drug among the ones considered in this paper. This is also what was seen in Figure 2.9. The red regions in Figure 2.11 correspond to a PTEN fault being active and the PI3K inhibitor LY294002 seems to keep the apoptosis ratio away from the red region despite the presence of PTEN faults. This adds to the argument that the cell survival pathway contributes to TRAIL resistance, and its inhibition increases TRAIL sensitivity.
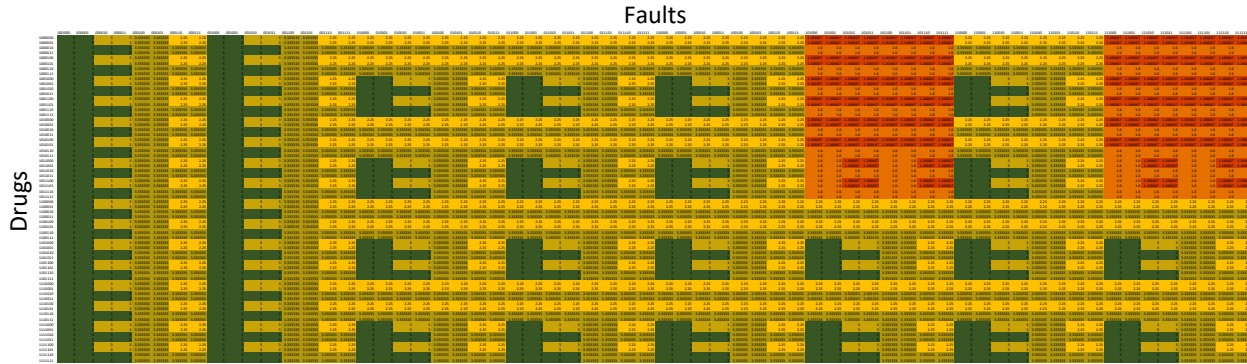
Figure 2.10: All possible combinations of faults and drugs when the input is TRAIL with Cryptotanshinone. Reprinted from Saraf 2018 ([1]).

The cell survival pathway is also known as the mTOR/PI3K/AKT pathway.

2.2.3 Experimental Results

The cellular apoptosis occurring in A375 melanoma cells with respect to time is displayed in Figure 2.12. The Y-axis shows the apoptotic fraction, which corresponds to the percentage of apoptosis occurring in the cell line in the given time [51]. Table 2.2 explains the legend in Figure 2.12 in greater detail.

Table 2.2: Legend for Figure 2.12. Reprinted from Saraf 2018 ([1]).

Abbreviation	Drug Combination
Cry	Cryptotanshinone $50\mu M$
+Ly	LY294002 $10\mu M+$ Cryptotanshinone $50\mu M$
+Tem	Temsirolimus $10\mu M+$ Cryptotanshinone $50\mu M$
+U0	U0126 $10\mu M+$ Cryptotanshinone $50\mu M$
+Lap	Lapatinib $10\mu M+$ Cryptotanshinone $50\mu M$
+SH	SH5-07 $10\mu M+$ Cryptotanshinone $50\mu M$
+AG	AG1024 $10\mu M+$ Cryptotanshinone $50\mu M$
Untreat	Untreated
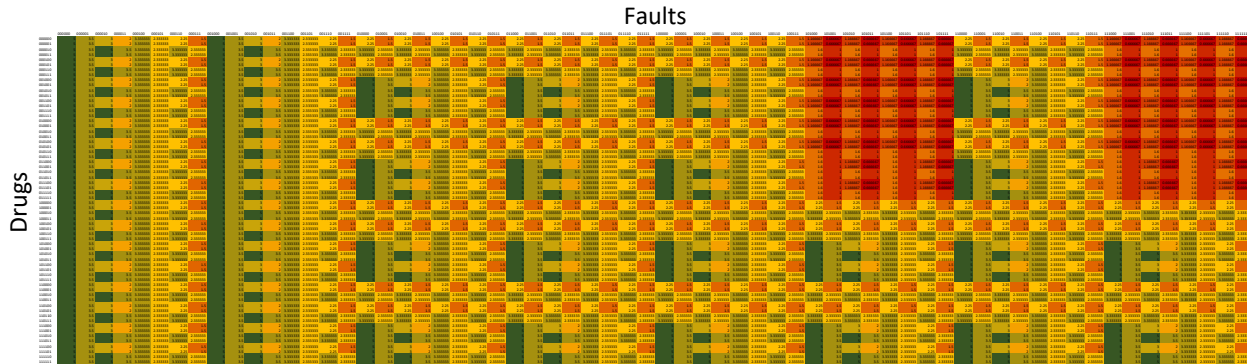
Figure 2.11: All possible combinations of faults and drugs when the input is TRAIL without Cryptotanshinone. Reprinted from Saraf 2018 ([1]).
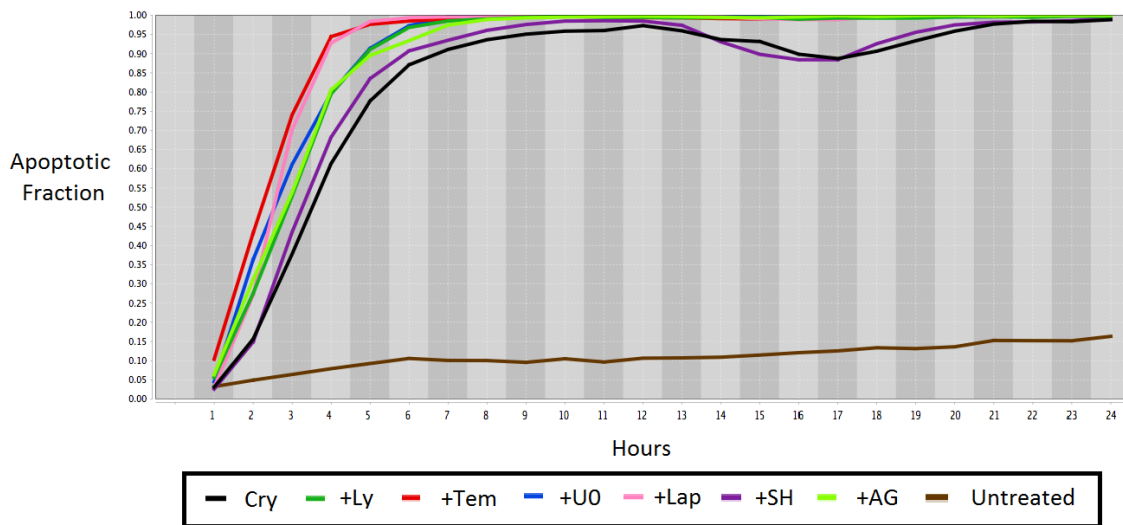
Figure 2.12: Experimental results for each single drug in combination with CT. Reprinted from Saraf 2018 ([1]).

24

It can be seen that CT in combination with the drugs one at a time is successfully inducing apoptosis in the melanoma cell lines. The final value of apoptosis is similar for each combination as is also shown in Figure 2.9.

3. OSTEOSARCOMA

3.1   Current State of Cancer Therapy for Osteosarcoma

Osteosarcoma (OS) is the most common primary malignant bone tumor of both children and pet canines. OS is characterized as a pediatric cancer since of the new cases diagnosed each year, more than half are children or adolescents [52, 53].

The genetic mutations or pathway alterations that could be responsible for the pathogenesis of OS have not been identified, which makes development of targeted therapies difficult [54].

3.1.1   Key Intervention Points in Osteosarcoma

There is a large set of potential candidate genes which must be evaluated to characterize molecular targets in order to develop new strategies [55, 56]. Our approach to narrow the search space is two-pronged:

1. we study OS in dogs to identify statistically significant mutations that could be associated with the bone cancer.

2. we investigate the drugs that have been successful in clinical trials and evaluate their targets as potential intervention points.

3.1.1.1   Key Intervention Points in Canine Osteosarcoma

Genetically, osteosarcoma is the same in humans and canines; they share dysregulation of many of the same biological pathways [57, 58, 59]. The higher incidence and more rapid disease progression seen in pet dogs allows for faster and more cost effective data collection making them an excellent model for studying this disease for the mutual benefit of both the species [60].

An evaluation of OS in dogs tells us that the pathways involved in the glutathione and aspartate metabolism may have an important role to play in the early spread of this cancer [57]. We will incorporate the relevant interconnections and cross talk with the metabolic pathways into our model.

3.1.1.2 *Drugs Under Clinical Trial for Osteosarcoma*

Conventional drug therapies that target the mutated tumor suppressor pathways fail in the late stages of the clinical trials [61]. Recent success in OS therapy has been through trials that target the stemness pathways, namely Wnt/β-Catenin and Hedgehog pathways through the use of natural compounds. Sulforaphane is one of the natural compounds being used to treat OS cell lines; the drug increases the expression of death receptors and induces tumor necrosis factor (TNF)–related apoptosis-inducing ligand (TRAIL) apoptosis [56, 55, 62].

TRAIL therapy is a therapeutic strategy that inhibits tumor growth and increases chances of survival in preclinical studies for OS. Since TRAIL-induced cell death is known to only kill cancer cells and not affect normal cells, it is one of the popular emerging strategies in pediatric cancer care and another pathway that warrants investigation [62, 63]. We model the stemness pathways and their interaction with the various pathways involved in TRAIL sensitivity for OS.

3.1.2 Drug Intervention in Osteosarcoma

We study the action of Cryptotanshinone (CT), a derivative of the herb Salvia milthorrhiza Bunge and a known STAT3 inhibitor that has been used to eradicate tumor-initiating cells in other cancers [64, 65, 32, 31]. Additionally, CT is known to be effective in increasing TRAIL cytotoxicity by upregulating death receptor 5 (DR5) and inducing cell death in cancer cells[30, 28]. Through its action on dynamin-related protein 1 (DRP1), CT controls mitochondrial function which could inhibit OS cell growth [66].

3.2 Theoretical Network Modeling and Experimental Results for Osteosarcoma

We use a Boolean network model to capture the causal interconnections between the different genes from the different biological pathways. The candidate biological pathways for OS, namely angiogenesis (JAK/STAT), immune system (KEAP1/NRF2), inflammation(NKκB), hypoxia (H1F1α), stemness (Wnt/β-Catenin and Hedgehog) and the metabolic pathways, are all well documented [7, 5, 6]. Some of the interconnections derived during modeling these pathways are based on the interpretation of different research papers [56, 54, 62, 67, 47, 48, 2, 68, 69, 24, 44, 43, 42, 41, 13, 50, 45, 70, 66] by the author of the present dissertation. We consider only a subset of all possible interconnections and signaling pathways in the cell, since the cancer of interest here is OS.

3.2.1 Results and Discusions

For clarity of exposition, the entire Boolean network has been divided into six components. The legend and color scheme given in Fig. 3.1 applies to each component from Fig. 3.2 to Fig. 3.7; the crosstalk between the different pathways is denoted by the blue blocks. Fig 3.2 shows the cell survival pathways; this figure shows the activity points of many conventional drugs. Cancer cells hijack the cell survival mechanism to evade cell death and to promote the growth of the tumor. Fig. 3.3 shows the interconnections between the endoplasmic reticulum stress-activated pathway and cellular damage and their cumulative effect on the glutathione metabolism. The hypoxic (low oxygen) conditions associated with cancer cause endoplasmic reticulum stress to initiate the unfolded protein response; the low oxygen condition also initiates the switch to anaerobic metabolism [69, 57]. The stemness pathways are modeled in Fig. 3.4; mesenchymal stem cells are controlled by stemness-related genes and could play an important role in osteosarcoma pathogenesis [64]. Hypoxia and angiogenesis pathways are displayed in Fig. 3.5, the gene STAT3 and its influence on the immune system, inflammation, angiogenesis as well as hypoxia can be studied in this figure. Fig. 3.6 and Fig. 3.7 show the extrinsic and mitochondrial apoptotic pathways respectively. The induction of TRAIL apoptosis by CT can be seen in Fig. 3.6.
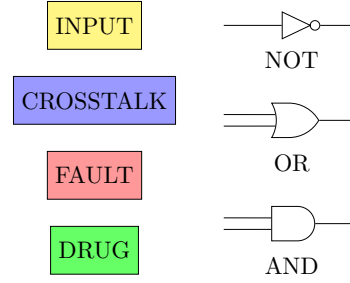
Figure 3.1: Legend and color scheme for Fig. 3.2-Fig. 3.7.

The static Boolean network considered in this work is subject to a certain set of inputs whose effect on the network can be evaluated through a set of outputs; the input and output vectors are given in Eq. 3.1 and Eq. 3.2 below. The inputs are a mix of growth factors, interleukins, interferons and stress signals which activate the pathways relevant to the pathogenesis of OS. The value of these inputs manipulate cell growth and death by controlling the state of the nodes downstream. The outputs are a set of genes that give information about cell death or apoptosis. The outputs can be classified into two categories: pro-apoptotic and anti-apoptotic, which promote and inhibit cell death respectively. The Table. 3.1 shows this classification of outputs. The fate of the cell depends on the value of these apoptotic factors.

$$\text{Inputs} = [\text{IGF}, \text{TRAIL}, \text{CaLM}, \text{EGF}, \text{TNF}\alpha,$$
$$\text{IL6}, \text{TGF}\beta, \text{IFN}, \text{Hh}, \text{WNT}, \text{cAMP}, \text{ROS}] \tag{3.1}$$

$$\text{Outputs} = [\text{BAKX}, \text{BAD}, \text{CASP8}, \text{CASP12}, \text{BID},$$
$$\text{BIM}, \text{STING}, \text{DRP1}, \text{BCL2}, \text{BCLxL},$$
$$\text{MCL1}, \text{XIAP}, \text{XBP1}, \text{survivin}, \text{EPO}, \text{A1}] \tag{3.2}$$

We consider a total of 7 faults in our network. PTEN, p53, MDM2 and CXCR4 mutations are commonly found in OS cell lines; PTEN and CXCR4 faults can lead to a decrease in TRAIL
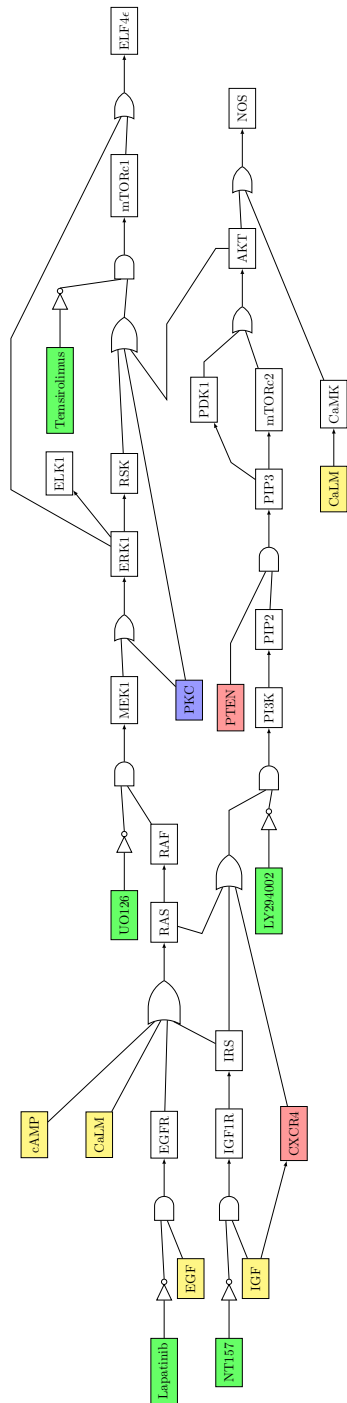
Figure 3.2: Cellular survival pathways.
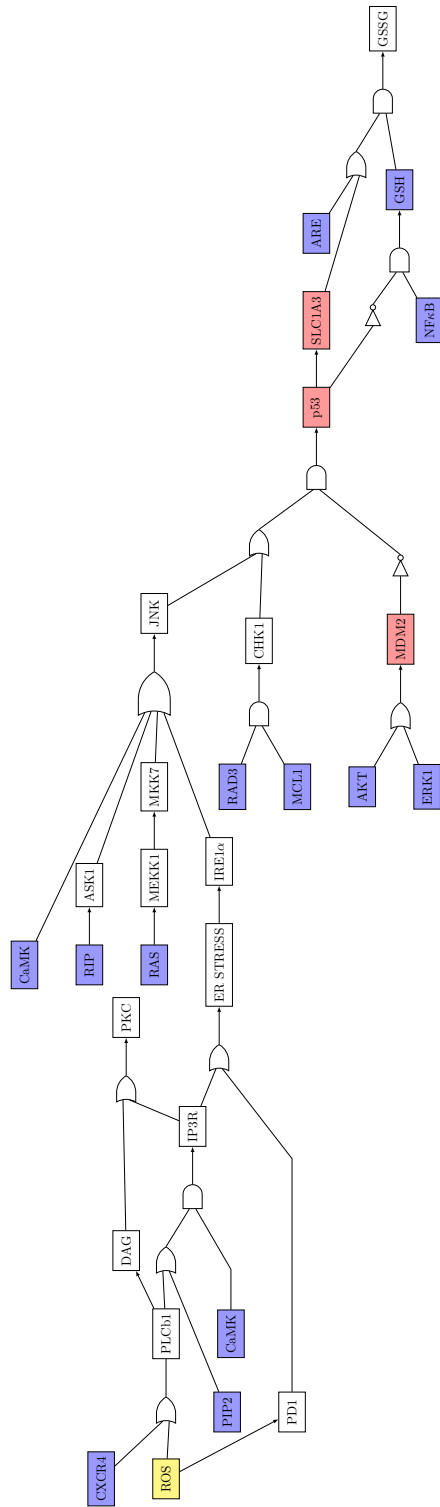
Figure 3.3: Endoplasmic reticulum stress-related pathways and their interconnections with cellular damage and the glutathione metabolism.
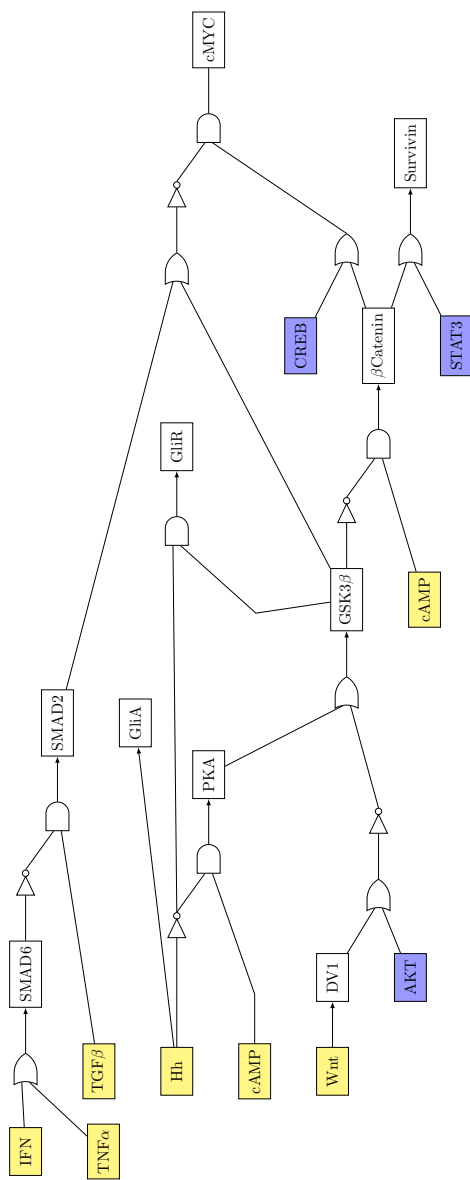
Figure 3.4: Stemness pathways
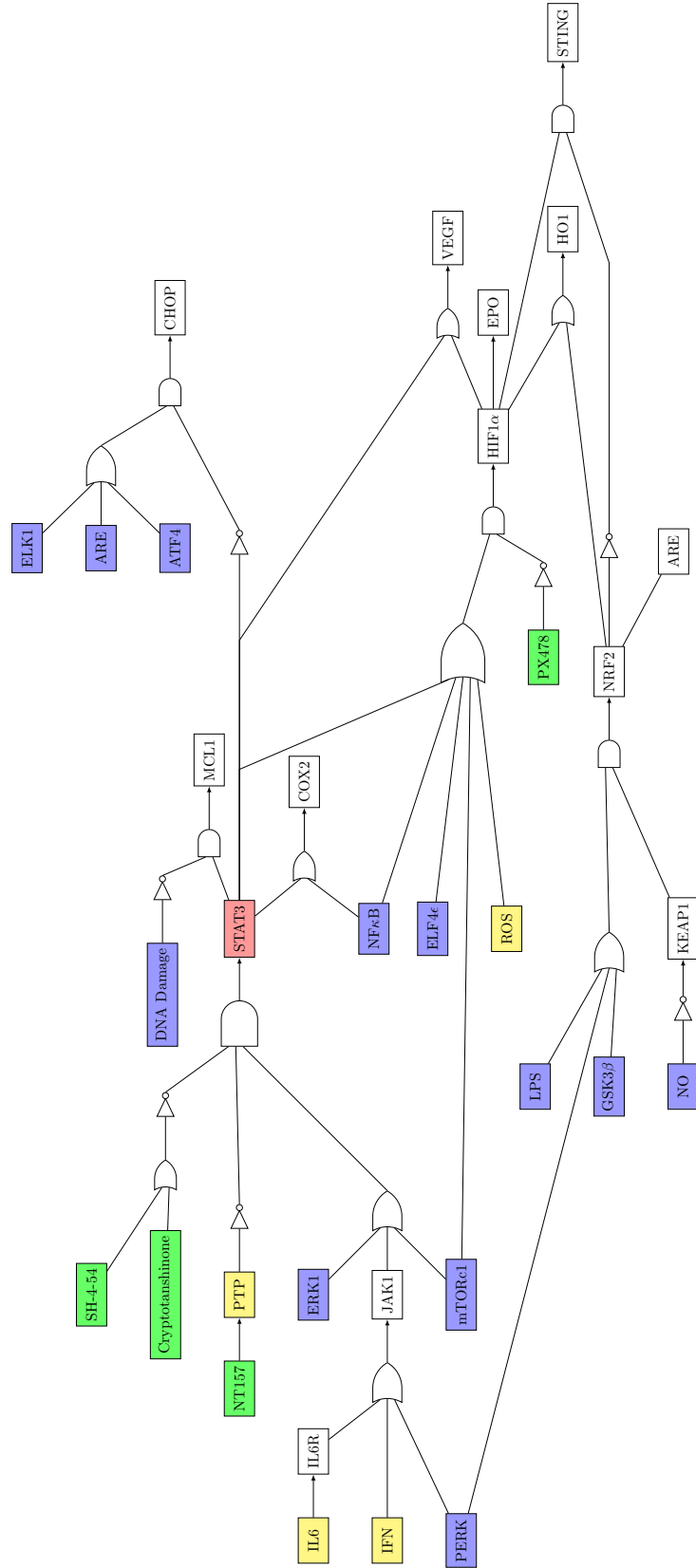
Figure 3.5: Hypoxia and angiogenesis pathway and their crosstalk with the immune system
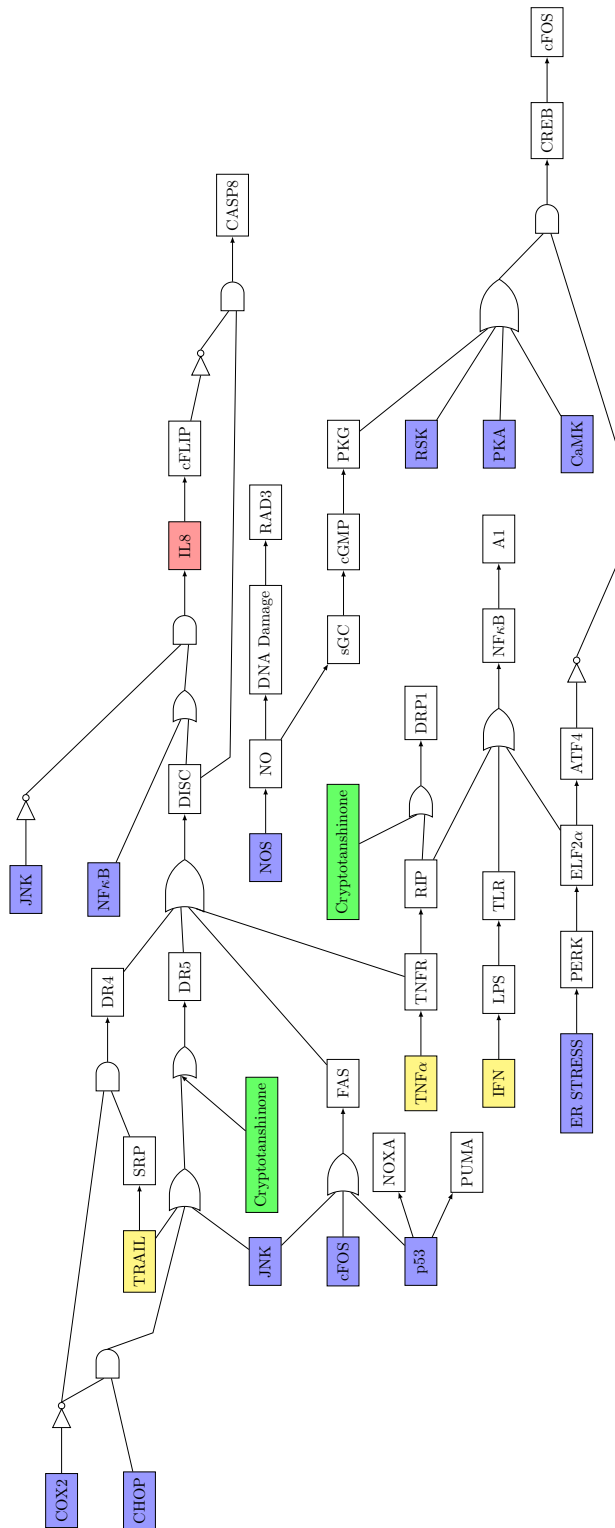
Figure 3.6: Extrinsic apoptosis
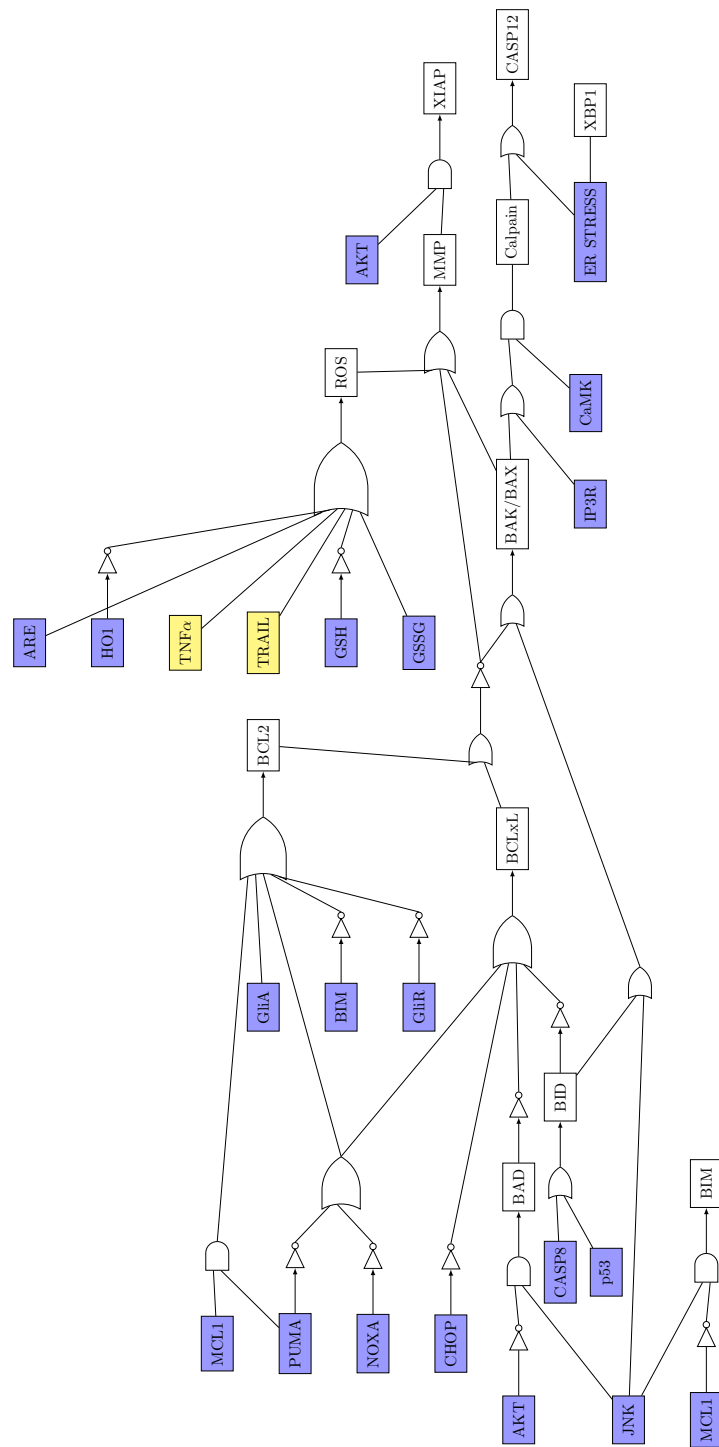
Figure 3.7: Mitochondrial apoptosis

Table 3.1: Apoptotic factors

Pro-apoptotic factors	Anti-apoptotic factors
BAK/BAX	BCL2
BAD	BCLxL
CASP8	MCL1
CASP12	XIAP
BID	XBP1
BIM	survivin
STING	EPO
DRP1	A1

Table 3.2: Faults in the Boolean network

Fault	Type
CXCR4	Stuck at 1
SLC1A3	Stuck at 0
IL8	Stuck at 0
MDM2	Stuck at 1
p53	Stuck at 0
PTEN	Stuck at 0
STAT3	Stuck at 1

sensitivity [61, 54, 56, 71, 12]. OS cell survival and drug resistance can be attributed to STAT3 overexpression, which can be characterized as a stuck-at-1 fault [64]. Furthermore, the study of canine gene expression identifies SLC1A3 and IL8 as the two mutations that could be responsible for OS progression in humans and dogs [57]. The faults and their corresponding types are displayed in Table 3.2 and the fault vector can be seen in Eq. 3.3. The components in the fault vector are either one or zero depending on whether a particular fault is present or not. A one in the fault vector denotes a stuck-at-0 or stuck-at-1 fault, whichever is applicable for that particular gene. For example, if the fault vector is $[0, 0, 0, 0, 1]$, this implies that the STAT3 gene is mutated. Since it is a stuck-at-one type of fault, it means that STAT3 is being constitutively expressed.

$$\text{Faults} = [\text{CXCR4}, \text{SLC1A3}, \text{IL8}, \text{MDM2}, \text{p53}, \text{DR5}, \text{STAT3}] \qquad (3.3)$$

Table 3.3: Drugs with their activity points

Abbreviation	Drug	Target
Cry	Cryptotanshinone	STAT3, DR5
Ly	LY294002	PI3K
Lap	Lapatinib	EGFR
NT	NT157	PTP
SH	SH-4-54	STAT3
Tem	Temsirolimus	mTOR
U0	U0126	MEK1
PX	PX-478	HIF1α

The drugs with their activity points are shown in Table 3.3 and the components of the drug vector are given in Eq. 3.4.

$$\text{Drugs} = [\text{Cry}, \text{Ly}, \text{Lap}, \text{NT}, \text{SH}, \text{Temsirolimus}, \text{UO126}, \text{PX}] \tag{3.4}$$

A one in the ith column of the drug vector indicates that the ith drug is applied and vice versa. We evaluate combinations of Cryptotanshinone with the other drugs, since a major goal of this work is to evaluate CT's action on OS cells. Since there are seven other drugs in the vector, a total of 2^7 drug combinations were tested. For instance, the drug vector $[1, 0, 0, 0, 0, 0, 0, 0]$ indicates that only Cryptotanshinone is applied.

3.2.2 Theoretical Simulation Results

We ran simulations under different combinations of drugs and faults to compare the results of the model and the biological experiment. We predict the theoretical drug efficacies of drug combinations with and without Cryptotanshinone. We fix the values of the inputs for all the simulations as $[1, 1, 0, 0, 0, 0, 0, 0, 0, 0, 0, 0, 0, 0]$, where the IGF and TRAIL inputs are active, since TRAIL sensitivity is of us interest to us. TRAIL sensitivity is the ability of a cancer cell to respond to death signals. TRAIL resistance is observed in OS cells and is said to occur when an active TRAIL input is unable to induce apoptosis in cancer cells [72]. IGF activates the PI3K/mTOR pathway which has been implicated in decreasing TRAIL cytotoxicity [12]. The metric used to

calculate the degree of apoptosis is given in Eq. 3.5.

$$\text{Apoptosis Ratio} = \frac{\sum \text{Pro-Apoptotic factors}}{\sum \text{Anti-Apoptotic factors}} \qquad (3.5)$$

The apoptosis ratio measures the relative change in cell death for each different set of inputs. The active faults and drugs will also affect the apoptosis ratio. We assume that all faults are active, i.e. the fault vector is $[1, 1, 1, 1, 1, 1, 1]$.

3.2.3   Experimental Results

Cellular apoptosis is tracked using high-content fluorescent protein reporter imaging with the previously immortalized ABRAMS canine OS cell line to study how it reacts to different combinations and concentrations of drugs. A two-part data processing technique is applied to extract the cell dynamics from the images. First, image processing is performed on the fluorescent images to recognize individual cells and quantify their transcription activity levels. Second, an algorithm for data representation summarizes the results into expression profiles in order to facilitate further evaluation [51]. This method produces a plot of cellular apoptosis versus time for a given drug combination.

3.2.3.1   CT is Effective at Restoring TRAIL Sensitivity

First, we compare the action of Cryptotanshinone alone with the action of the PI3K inhibitor LY294002. The cellular apoptosis occurring in ABRAMS OS cells with respect to time is displayed in Fig 3.8. The Y-axis shows the apoptotic fraction, which corresponds to the percentage of apoptosis occurring in the cell line in the given time. Table 3.4 explains the legend in Fig 3.8 in greater detail.   The curve in Fig. 3.8 shows the effect of CT and LY294002 on OS cells. It is clear from the Fig. 3.8 that Cryptotanshinone is more effective than LY294002 in inducing apotosis. The area under the curve for each of the curves in Fig. 3.8 is plotted in Fig. 3.9 as a bar graph for ease of comparison. Fig. 3.10 shows the simulated effect of the drugs CT and LY294002 on the Boolean network. The 'Untreated' condition is simulated by passing a drug vector of zeros. The Boolean network subject to Cryptotanshinone outputs a greater apotosis ratio than the one subject
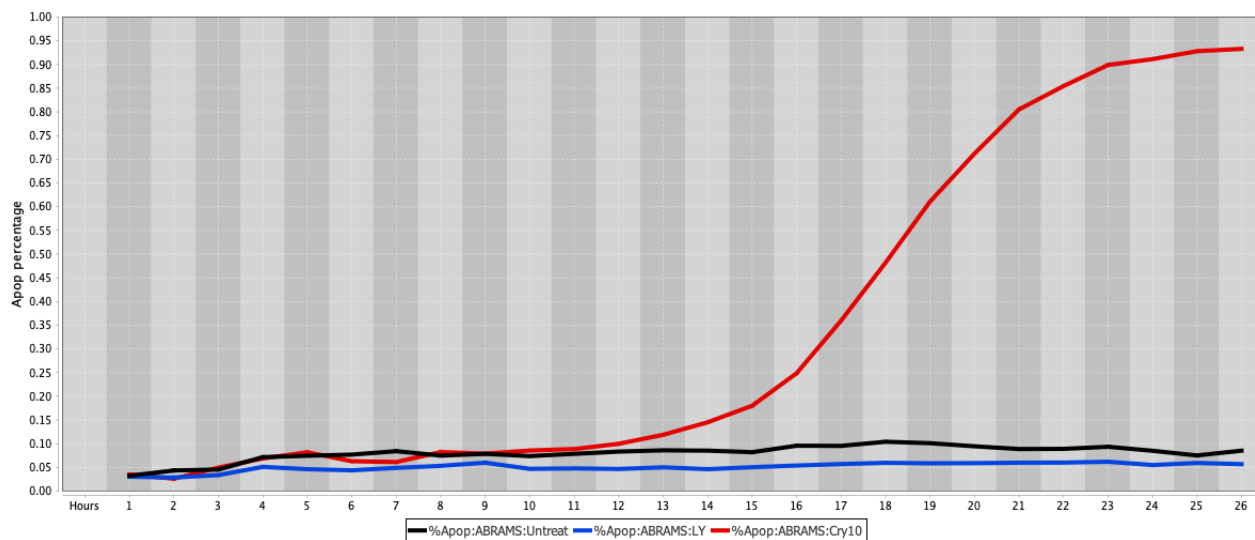
Figure 3.8: Experimental results comparing LY294002 with CT.

Table 3.4: Legend for Fig 3.8

Abbreviation	Drug Combination
Cry	Cryptotanshinone $10\mu M$
Ly	LY294002 $10\mu M$
Untreat	Untreated

to LY294002. Upon comparison of the Fig. 3.9 and Fig. 3.10, it is evident that the two graphs are similar. The simulation shows us that CT can induce apoptosis on its own, whereas the inhibition of PI3K alone is not sufficient to restore TRAIL cytotoxicity.

3.2.3.2 *Inhibition of the PI3K/mTOR Pathway Boosts CT's Action*

Next, we test the combination of Cryptotanshinone with one drug at a time. We have five drugs in different concentrations mixed with equal dosage of Cryptotanshinone. The cellular apoptosis occurring in ABRAMS OS cells with these conditions is displayed in Fig 3.11. Table 3.5 explains the legend in Fig 3.11 in greater detail.   The curve in Fig. 3.11 shows how all the drug combinations successfully lead to apoptosis. Note that since every combination has Cryptotanshinone as a component, it could imply that Cryptotanshinone is responsible for the effectiveness of the drug
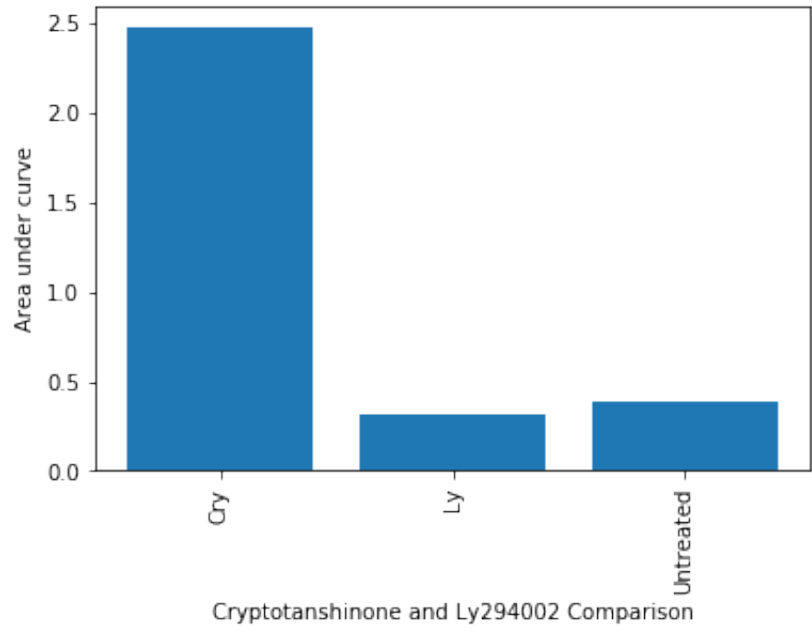
Figure 3.9: Area under the curve in Fig. 3.8.
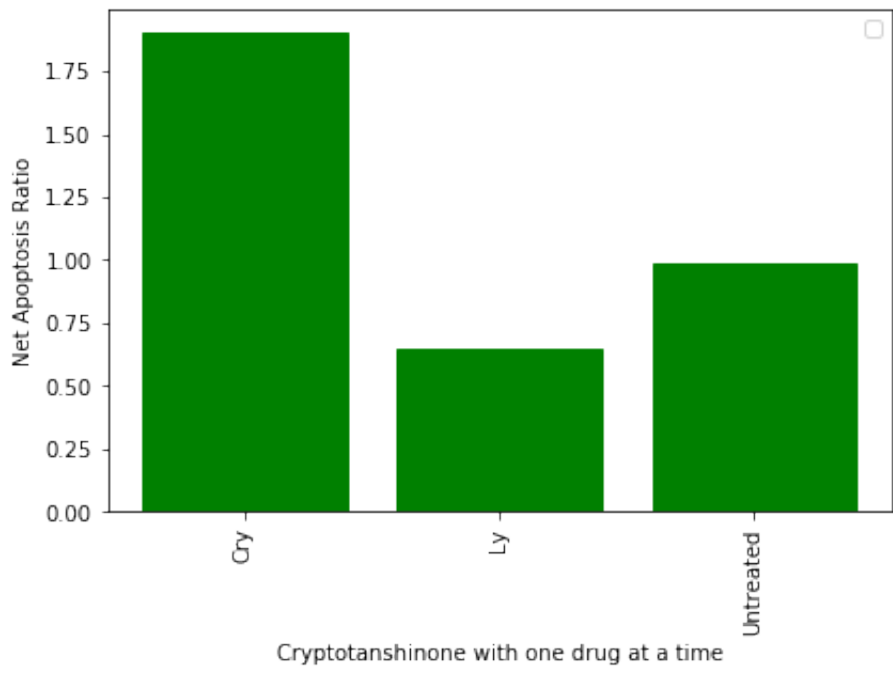
Figure 3.10: Simulation results comparing LY294002 with CT.
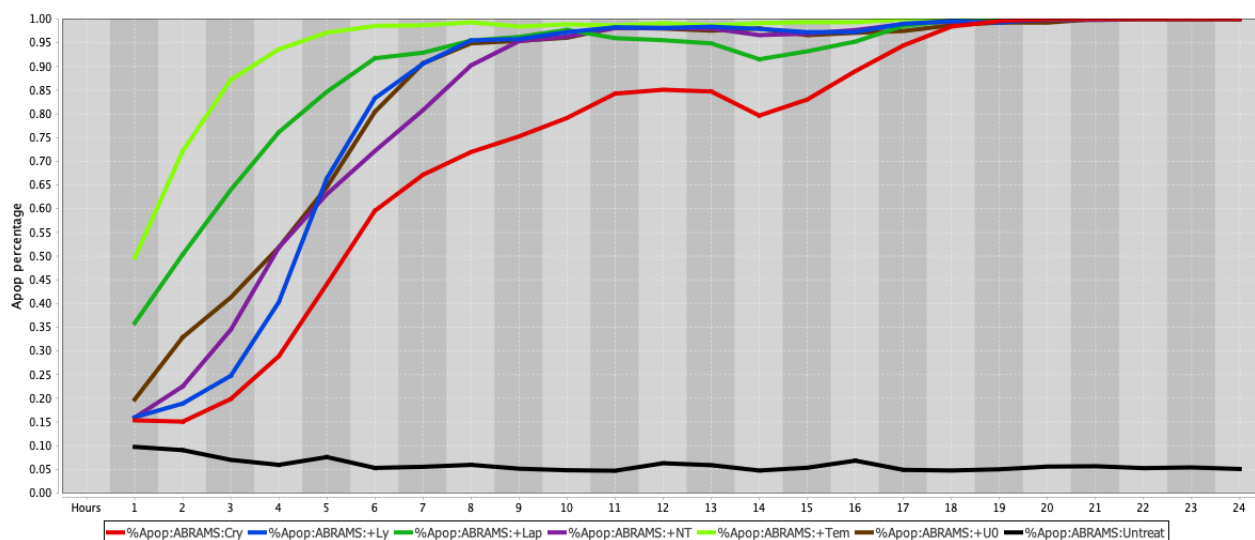
Figure 3.11: Experimental results for each single drug in combination with CT.

Table 3.5: Legend for Fig 3.11

Abbreviation	Drug Combination
Cry	Cryptotanshinone $50\mu M$
+Ly	LY294002 $10\mu M+$ Cryptotanshinone $50\mu M$
+Lap	Lapatinib $5\mu M+$ Cryptotanshinone $50\mu M$
+NT	NT157 $10\mu M+$ Cryptotanshinone $50\mu M$
+Tem	Temsirolimus $10\mu M+$ Cryptotanshinone $50\mu M$
+U0	U0126 $10\mu M+$ Cryptotanshinone $50\mu M$
Untreat	Untreated

cocktail. We can see that the combination of CT with Temsirolimus, the MTOR inhibitor is the most effective. The area under the curve for each of the curves in Fig. 3.11 is plotted in Fig. 3.12 as a bar graph for ease of comparison. The output of the Boolean network shows that LY294002, the PI3K inhibitor in combination with CT is the best performing combination. We can also see that all the combinations lead to high values of the apoptosis ratio. Both Fig. 3.12 and Fig. 3.13 seem to indicate that the inhibition of PI3K/mTOR pathway amplifies the effect of CT and helps overcome TRAIL resistance.
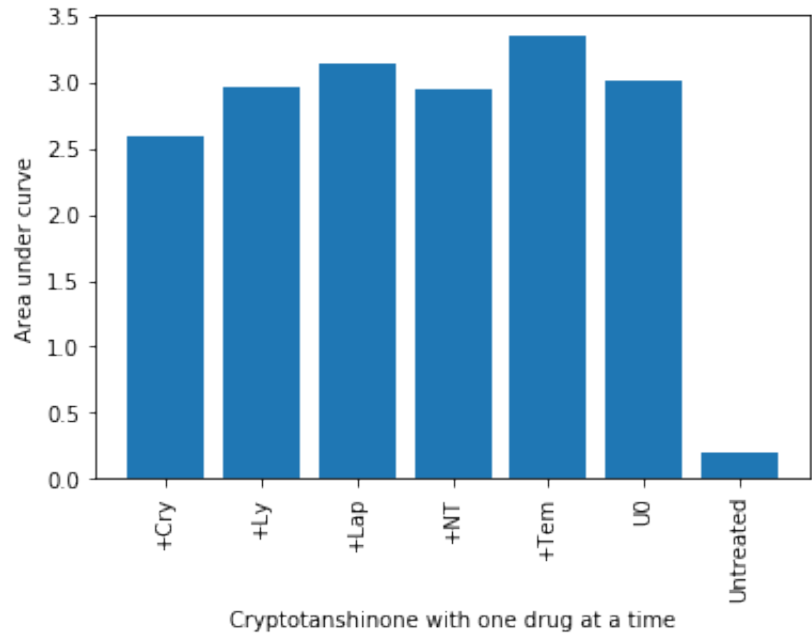
Figure 3.12: Area under the curve in Fig. 3.11.
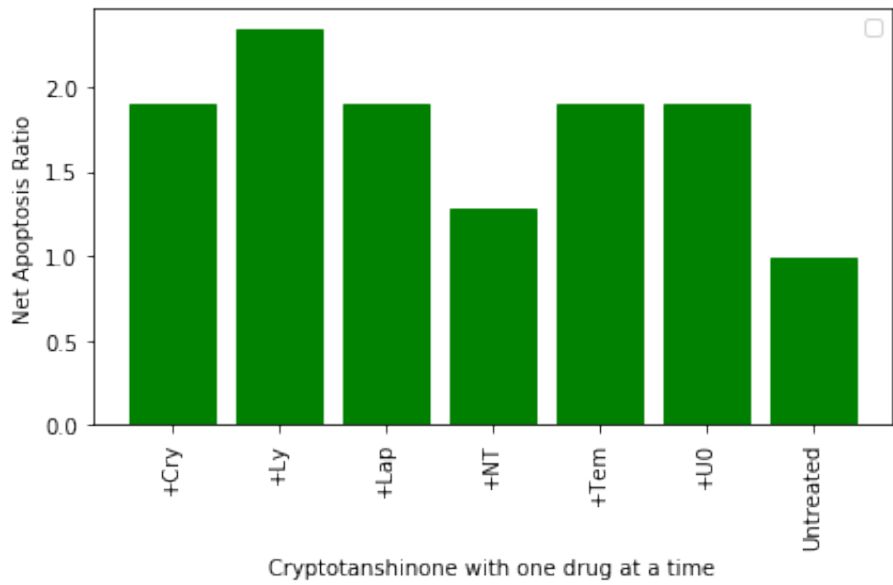
Figure 3.13: Simulation results for each single drug in combination with Cryptotanshinone.

3.2.3.3   *HIF1-alpha is a Key Intervention Point in OS Pathways*

The third experiment was performed with Cryptotanshinone and other two drugs at a time. All the drug combinations in this experiment have Cryptotanshinone and HO-3867 (a STAT3 inhibitor) in the mix. The cellular apoptosis occurring in ABRAMS OS cells with respect to time is displayed in Fig 3.14. Table 3.6 explains the legend in Fig 3.14 in greater detail.   As seen in Fig 3.14, both
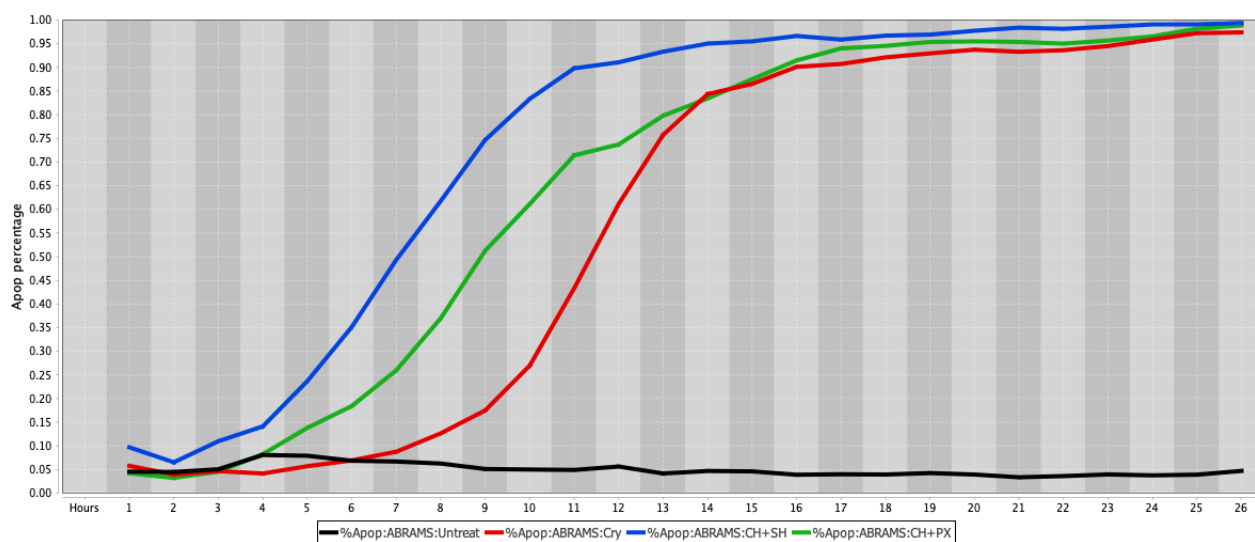
Figure 3.14: Experimental results comparing PX478 with CT.

Table 3.6: Legend for Fig 3.14

Abbreviation	Drug Combination
Cry	Cryptotanshinone $20\mu M$
+PX	PX478 $10\mu M$+ Cryptotanshinone $25\mu M$ + HO-3867 $10\mu M$
+SH	SH-4-54 $5\mu M$+ Cryptotanshinone $50\mu M$ + HO-3867 $10\mu M$
Untreat	Untreated

the drug combinations successfully induce cell death in the OS cell line, and the combination with PX-478 is slightly more effective than the one with SH-4-54. The area under the curve for each of
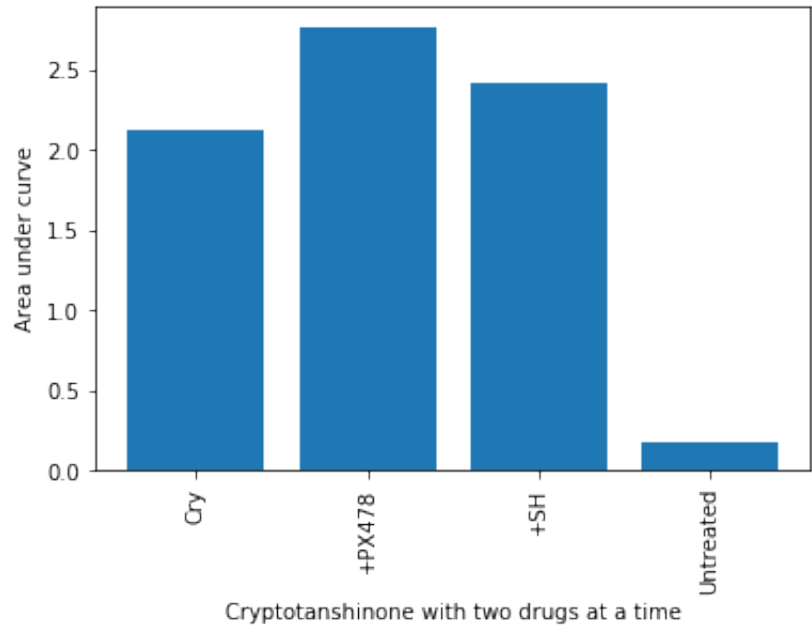
Figure 3.15: Area under the curve in Fig. 3.14.
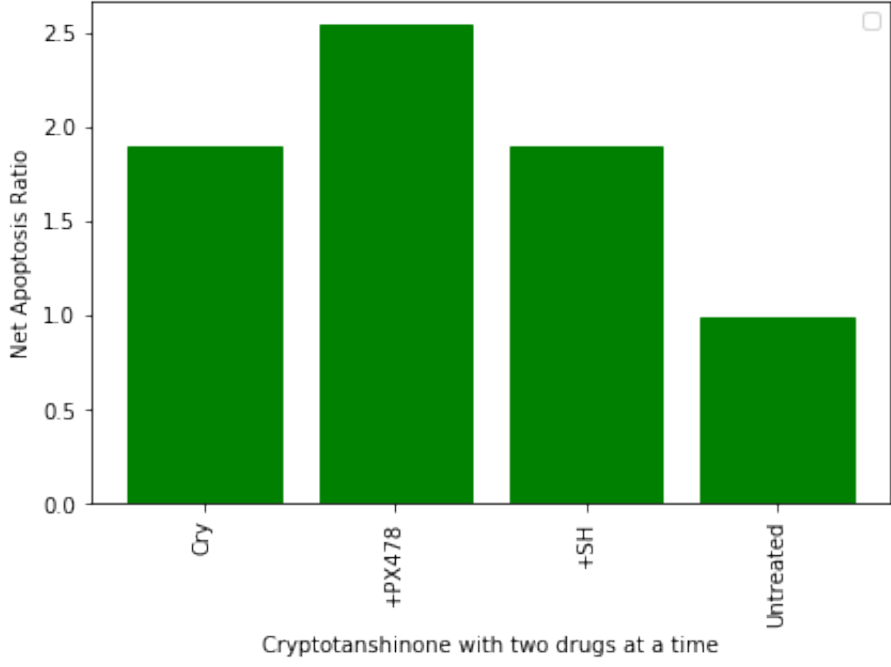
Figure 3.16: Simulation results comparing PX478 with CT.
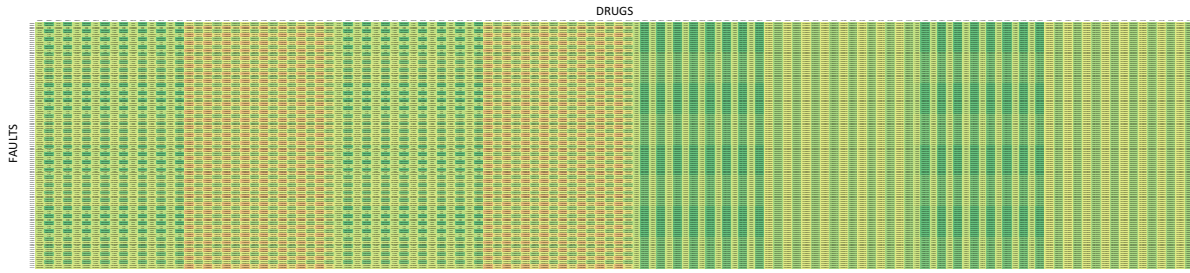
Figure 3.17: All possible drug Combinations with Cryptotanshinone.

the curves in Fig. 3.14 is plotted in Fig. 3.15 as a bar graph for ease of comparison. The simulation results show a similar trend as the one in the biological experiment. The results of this experiment show that inhibition of HIF1α enhances the activity of CT. The Boolean model predicts that the combination of CT with PX-478 is the best combination with two other drugs at a time, which implies that HIF1α is a significant intervention point in OS treatment.

3.2.4 Prediction of Drug Efficacies

The final simulation was performed to test the effect of all possible combinations of faults and drugs with and without Cryptotanshinone. Fig. 3.17 shows all the drug combinations containing CT and Fig. 3.18 considers the possible combinations of drugs without CT. The cells that are green indicate high levels of apoptosis (6.5) and the red cells denote low levels of apoptosis (0.3). Fig 3.18 has several red cells, implying that most of the conventional drug combinations fail to induce apoptosis. Fig. 3.17 has no red cells, which implies that no combination with CT in mix has a low apoptosis ratio. Our model predicts that every combination with CT should be able to increase TRAIL sensitivity and induce robust cell death in OS cells despite the presence of faults.

3.2.5 Further Biological Experimentation

We predict the best drug cocktail with three drugs for treatment of OS. The ranking of the drug combination is performed on the basis of the corresponding apoptosis ratio. We ran a simulation for drug combinations of three drugs at a time, with or without Cryptotanshinone.

The top drug combinations with CT as seen in Figure. 3.19 are given in Table. 3.7 and the top
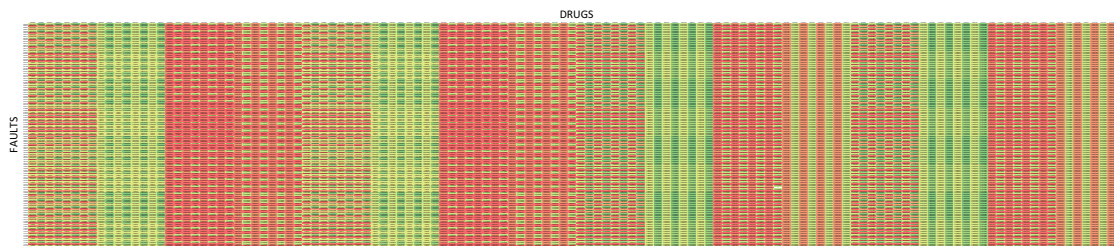
Figure 3.18: All possible drug combinations without Cryptotanshinone.
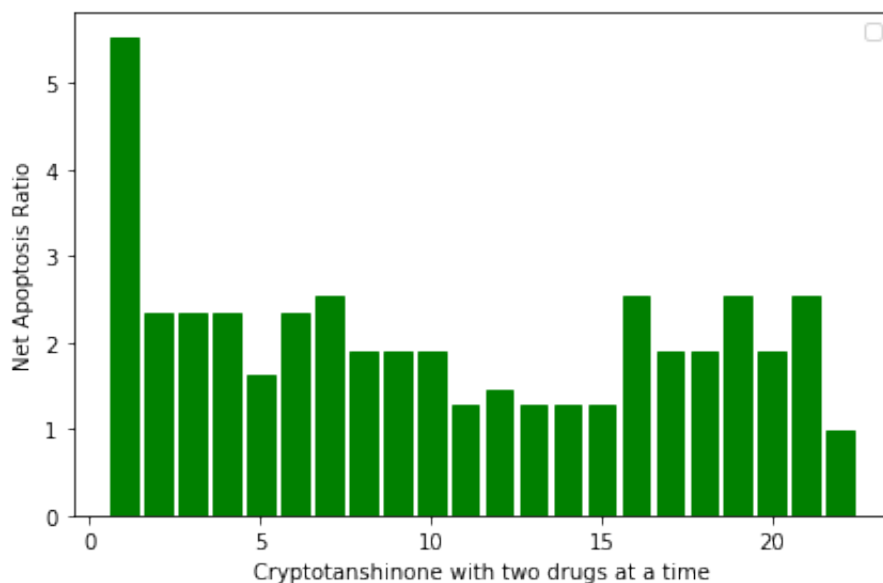
Figure 3.19: Drug combinations with Cryptotanshinone and two additional drugs.

drug combinations without CT as seen in Figure. 3.20 are given in Table. 3.8.

Table 3.7: Best drug combination with CT.

Drug Combination	Apoptosis Ratio
CT + PX478 + Ly294002	5.53

Biological experimentation was performed to compare the combinations of CT+PX478+Ly294002, SH454+Ly294002+PX478 and CT+SH454 to see whether CT outperforms SH-4-54. We measured
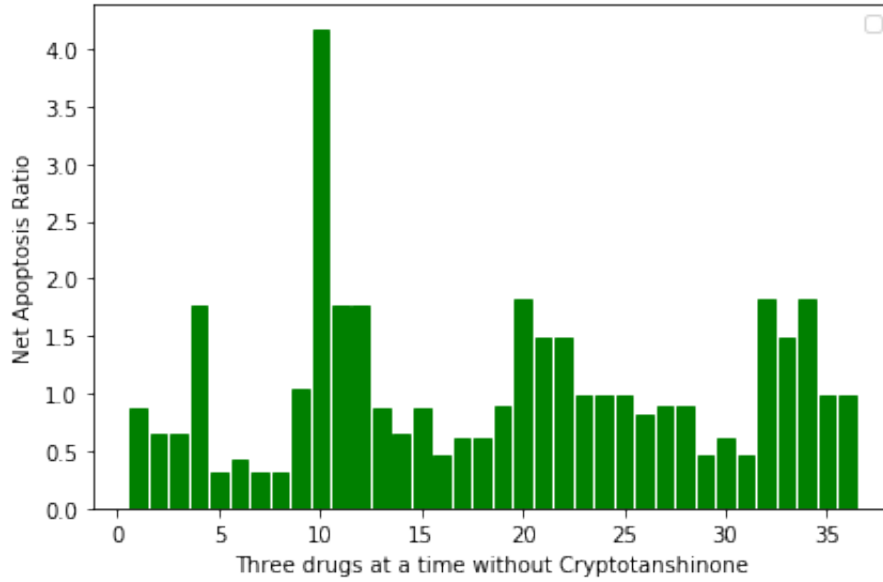
Figure 3.20: Drug combinations without Cryptotanshinone.

Table 3.8: Best drug combination without CT.

Drug Combination	Apoptosis Ratio
SH454 + Ly294002 + PX478	4.17

the percent survival rate of the Abrams canine OS cell line when it was subjected to a drug combination. Percent survival is inversely proportional to the efficacy of the drug combination. The results of the experiment can be seen in Figure. 3.21. The resultant ranking is listed in Table.3.9.

Table 3.9: Ranking of the drug combinations in terms of efficacy.

Drug Combination	Rank
CT + Ly294002 + PX478	1
CT + SH454	2
SH454 + Ly294002 + PX478	3

It can be seen that CT + Ly294002 + PX478 performs better than SH454 + Ly294002 + PX478, which implies that the success of this drug combination can be attributed to the effectiveness of

47
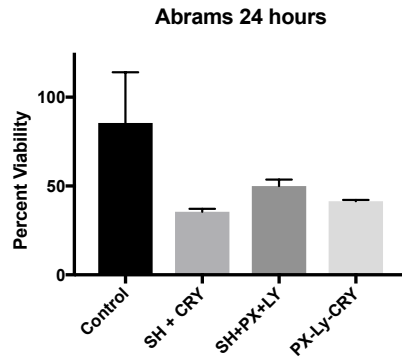
Abrams 24 hours

Figure 1: Percent survival of Abrams canine OS cell line after exposure to SH4-54 (5 uM), PX—478 (25 uM), LY2494002 (10 uM) and Cryptotanshinone (20 uM) after 24 hours of incubation. The SH + CRY treatment group was the most effect combination (mean percent viability 35.4% (SEM 0.55)) and was significantly lower than the control (p<0.0001) and the SH+PX+LY (p=0.0017) treatment groups. The PX+LY+CRY treatment group was the next most effective combination with mean viability of 41.37% (SEM 0.24) and was significantly lower than the control (mean viability 85.5% (SEM 9.5), p=0.02). The SH+PX+LY treatment group had a mean viability of 49.93% (SEM 1.2) and was not signficantly different from the control (p>0.99).
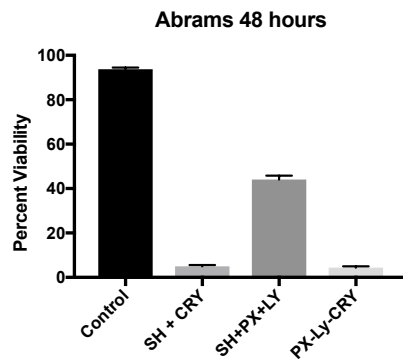
Abrams 48 hours

Figure 2: Percent survival of Abrams canine OS cell line after exposure to SH4-54 (5 uM), PX-478 (25 uM), LY2494002 (10 uM) and Cryptotanshinone (20 uM) after 48 hours of incubation. The PX+LY+CRY treatment group was the most effect combination (mean percent viability 4.34% (SEM 0.2)) and was significantly lower than the control (p<0.0001) and the SH+PX+LY (p=0.0076) treatment groups. The SH+CRY treatment group was the next most effective combination with mean viability of 4.95% (SEM 0.2) and was significantly lower than the control (mean viability 93.67% (SEM 0.26), p=0.0003). The SH+PX+LY treatment group had a mean viability of 44% (SEM 0.6) and was not significantly different from the control (p>0.42).

Figure 3.21: Biological experimentation to prioritize drug combinations on the basis of percent survival.

CT. It is evident from the results of the biological experiment that CT outperforms SH-4-54. Next, it can also be seen that CT + SH454 is a close second, which makes an even stronger case for CT as a promising drug for treatment of OS.

4.   GLIOBLASTOMA

4.1   Current State of Cancer Therapy for Glioblastoma

Glioblastoma or Glioblastoma Multiforme (GBM) is the most aggressive primary brain tumor with median overall survival (OS) of 14.6 months to 20.9 months in clinical trial setting and 11 months in all GBM population [73, 74] Current standard of care (SOC) treatments for GBM include maximum safe surgical resection, radiation, temozolomide (TMZ) chemotherapy and recently FDA approved tumor treating fields (Optune) for newly diagnosed patients as well as bevacizumab (Avastin) for recurrent disease [74, 75] However, GBM still stays as one of the most challenging cancers to treat due to its complexity or tumor heterogeneity, infiltrative nature and low efficacy of current treatment modalities which results in short-term survival rate. Therefore, novel approaches in the field of GBM drug discovery are needed to overcome current challenges in medication results [76]

Few of the main challenges to GBM treatment are resistance to temozolomide and recurrence of the cancer after radiation therapy. Understanding the genetic causes of this resistance to temozolomide is essential while designing therapies to robustly kill GBM tumor cells [77]. Studying the genetic makeup of GBM tumors is also essential while choosing drug combinations for post-radiation chemotherapy. By prioritizing the key genetic targets involved in the progression of GBM, the best drug combination can be predicted.

4.2 Theoretical Network Modeling for Glioblastoma

To aid the design of targeted therapy for GBM, it is necessary to model the cell signaling pathways involved in the development of the cancer. The biological pathways responsible for cell survival and proliferation are dysfunctional in GBM. Genetic aberrations in the cell cycle such as those originating from mutations in CDK2NA, p53, PTEN and EGFR are commonly found in GBM cell lines [78]. Additionally, genes associated with the Fas pathway, that is responsible for extrinsic apoptosis, are also a feature of GBM tumors. Isocitrate dehydrogenase (IDH) mutations can determine prognosis of a GBM patient and the involvement of IDH means the involvement of hypoxia-related and anaerobic metabolic pathways [78, 79]. Finally, the resistance to TMZ can be attributed to the DNA repair pathway which governs the methylation of Methylguanine-DNA Methyltransferase (MGMT); this motivates the investigation of DNA methylation and histone deacetylation pathways [33, 34]. The Boolean network model for GBM should include the interconnection between these pathways and the other pathways known to be active in cancer cells like the calcium signalling, endoplasmic reticulum stress-related and stemness (Wnt, Hedgehog and Notch) pathways [6, 7, 5].

Our objective is to show the effect of a gene on cancer cell fate. If a particular target gene or drug is said to be effective in terms of cancer treatment, it should have at least one of the following qualities :

- it should robustly kill cancer cells.

- it should stymie cancer cell growth or proliferation.

- it should abate tumor invasion and metastasis.

- it should curb tumor angiogenesis.

- it should attack the tumor-initiating cells.

To study the effect of the various genes on cancer cell fate, we include the pathways responsible for angiogenesis, inflammation and mitochondrial apoptosis.

4.2.1 Theoretical Simulation Results

The static Boolean network in this work maps a set of inputs to a set of outputs; the input and output vectors are given in Eq. 4.1 and Eq. 4.2 below. The inputs to the Boolean network are the growth factors, cytokines and extracellular stimulants relevant to the development of GBM. A change in input can cause a change in the output metric. The outputs are a mixture of apoptosis factors as seen in Eq. 4.3 and genes involved in the cell cycle arrest shown in Eq. 4.4. For all vectors, i.e input, output, fault and drug vectors, a one in the ith column of the vector implies that the ith element is active.

$$\text{Inputs} = [\text{Shh}, \text{Wnt}, \text{GF}, \text{IL17}, \text{Cytokine}, \text{TNF}, \text{PSEN}, \text{TGFb}, \text{S1P}, \text{Antigen}, \tag{4.1}$$
$$\text{Dopamine}, \text{GABA}, \text{Ach}, \text{HT}, \text{PGE2}, \text{EDN1}, \text{Norepinephrine}, \text{F2},$$
$$\text{Estrogen}, \text{Testosterone}, \text{Progesterone}, \text{NF1}]$$

The Tables 4.1 and 4.2 shows the classification of the apoptotic and arrest factors respectively. The fate of the cell depends on the value of these apoptotic and arrest factors.

$$\text{Outputs} = [\text{Apoptotic Factors}, \text{ Arrest Factors}] \tag{4.2}$$

$$\text{Apoptotic Factors} = [\text{BAK}, \text{BAX}, \text{BID}, \text{NOXA}, \text{PUMA},$$
$$\text{CASP12}, \text{CASP8}, \text{DNADamage}] \tag{4.3}$$

$$\text{Arrest Factors} = [\text{DNADamage}, \text{CHK1}, \text{HDAC}, \text{CDK4}, \text{CCND1}, \text{AR}] \tag{4.4}$$

For clarity of exposition, the Boolean network is divided into 8 parts as shown in Figures 4.1 through 4.8. The yellow blocks in the figures represent the inputs to the cells, the magenta

Table 4.1: Apoptotic factors

Pro-apoptotic factors	Anti-apoptotic factors
BAK/BAX	BCL2
BID	BCLxL
NOXA	MCL1
PUMA	XIAP
CASP12	CFLIP
CASP8	TERT
DNADamage	

Table 4.2: Arrest factors

Pro-Arrest factors	Anti-Arrest factors
DNADamage	HDAC
CHK1	CDK4
	CCND1
	AR

blocks represent the genetic mutations commonly found in GBM cell lines and the blue blocks represent the interconnections between the different pathways. Figure. 4.1 shows the cell growth pathways and their cross talk with the stemness pathways namely Wnt-βCatenin, Hedgehog and Notch. The histone deacetylation pathway and its interaction with PI3K/mTOR and inflammation pathways is shown in Figure. 4.2. The output factors that control cell proliferation, cell cycle arrest, angiogenesis and cell death are found in Figure. 4.3, Figure. 4.4 and Figure. 4.5 respectively. The DNA damage and repair network in Figure. 4.6 captures the commonly occurring faults in GBM. Figure. 4.7 shows how the g-coupled protein receptors influence calcium signaling and cAMP-PKA pathway in the brain. The hypoxia and endoplasmic reticulum stress-related pathways are active in several cancers including GBM are shown in Figure. 4.8.
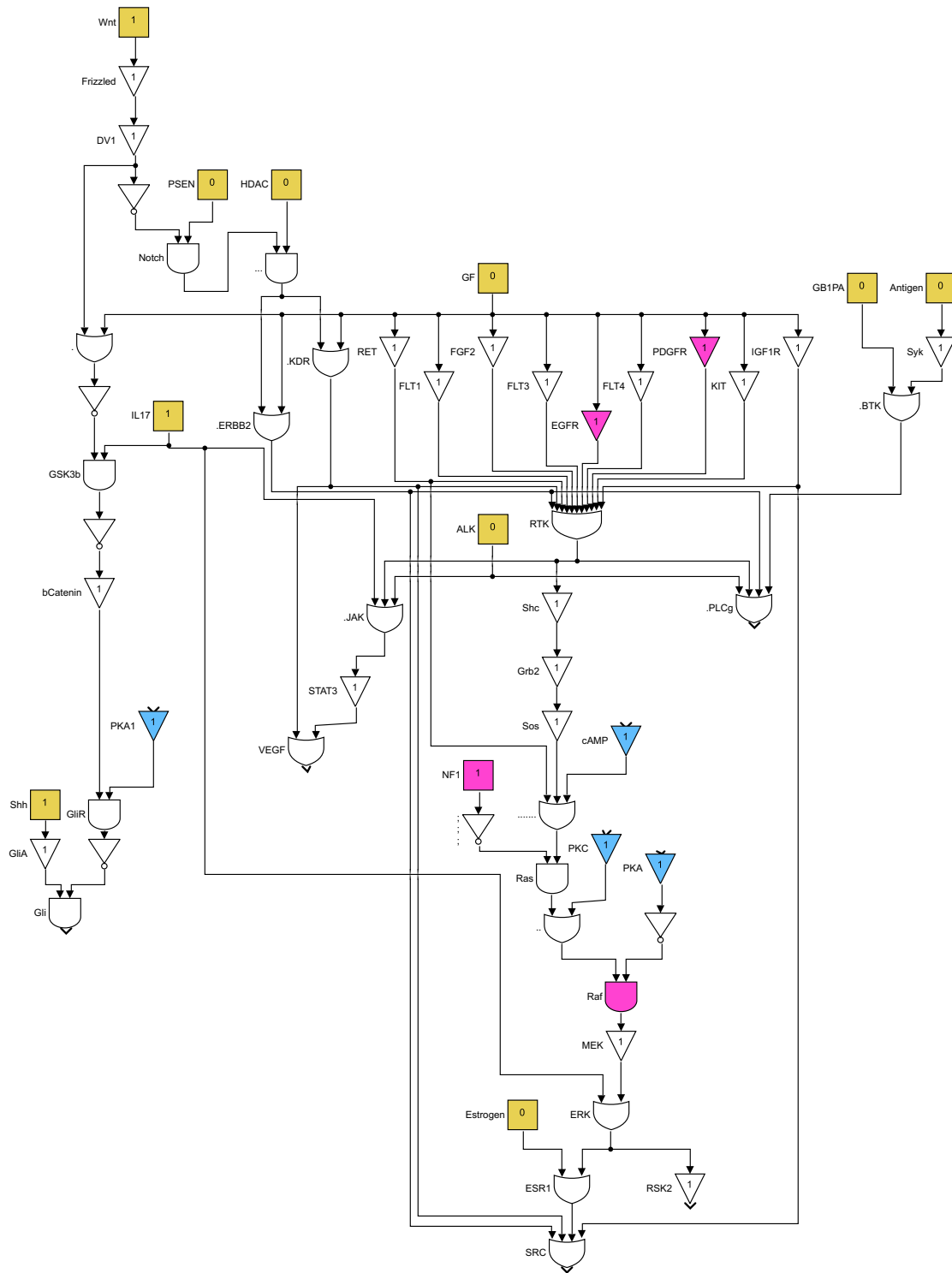
Figure 4.1: Cell growth and stemness pathways
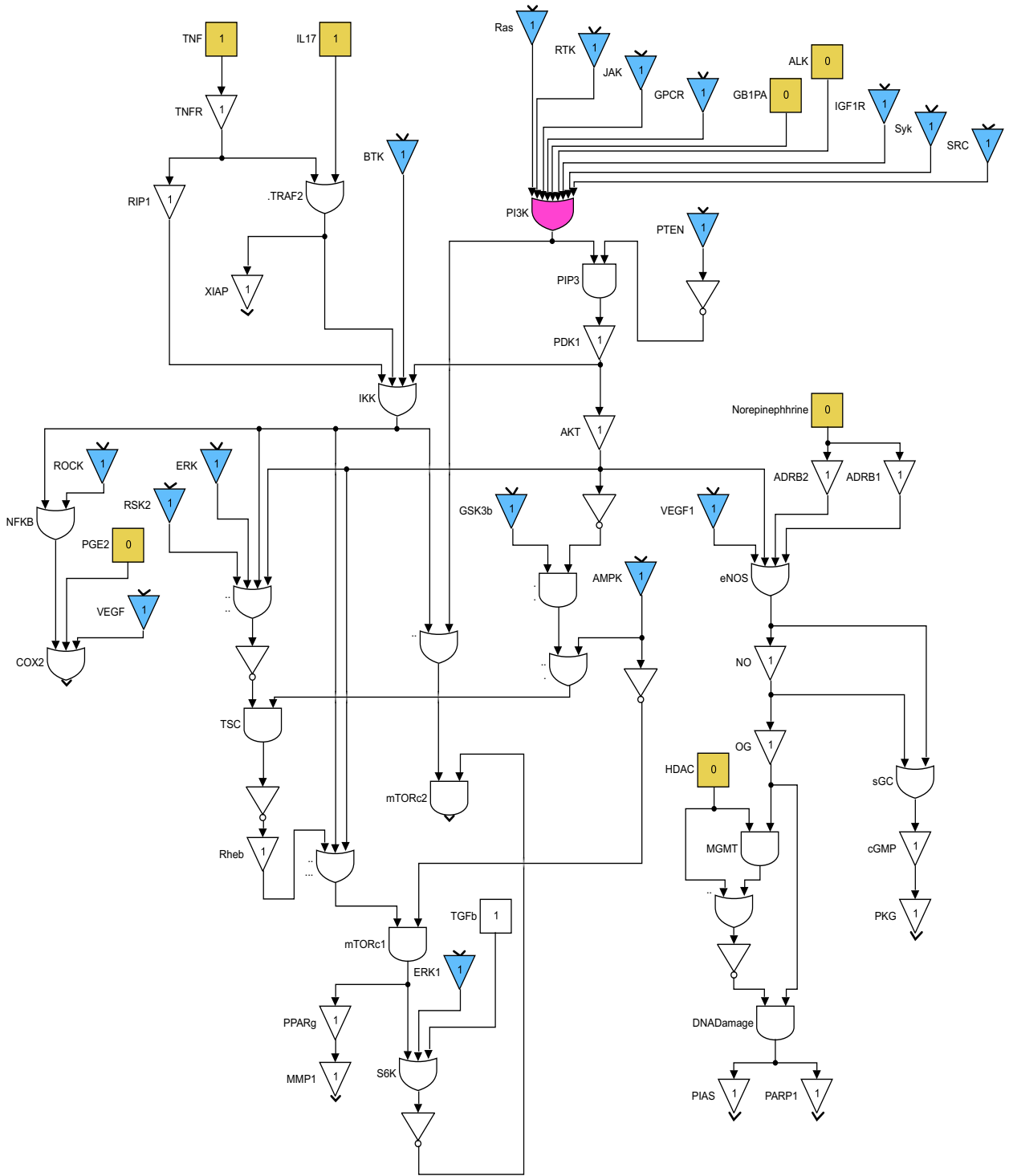
Figure 4.2: Cell survival, inflammation and histone deacetylation pathways

Figure 4.3: Apoptosis pathways

Output Metric

The output factors have been combined into one output metric to calculate the efficacy of the drug or target. The metric used is given in Eq. 4.7 and is a combination of the apoptosis ratio in
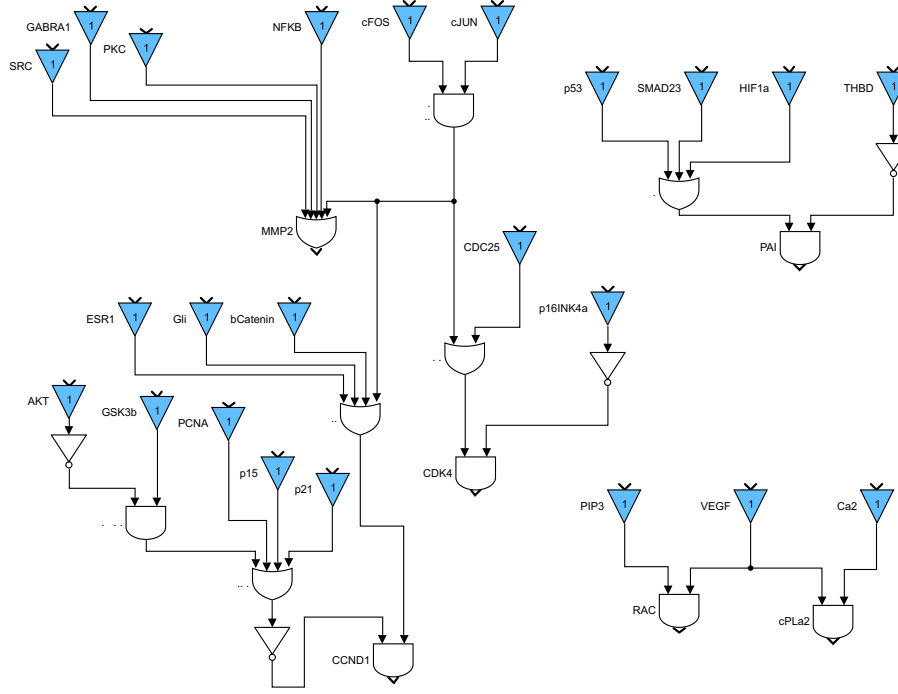
Figure 4.4: Cell cycle arrest and angiogenesis pathways

Eq. 4.5 and the arrest ratio in Eq. 4.6.

$$\text{Apoptosis Ratio} = \frac{\sum \text{Pro-Apoptotic factors}}{\sum \text{Anti-Apoptotic factors}} = R_{apo} \tag{4.5}$$

$$\text{Arrest Ratio} = \frac{\sum \text{Pro-Arrest factors}}{\sum \text{Anti-Arrest factors}} = R_{arr} \tag{4.6}$$

$$\text{Convex Sum} = \frac{N_{apo}}{N} R_{apo} + \frac{N_{arr}}{N} R_{arr} \tag{4.7}$$

The apoptosis ratio R_{apo} denotes the relative change in cell death for each different set of inputs and N_{apo} is the number of pro-apoptotic factors and anti-apoptotic factors in total. The arrest ratio R_{arr} denotes the relative change in cell cycle progression for each different set of inputs and N_{arr} is the number of pro-arrest factors and anti-arrest factors in total. Finally, $N = N_{apo} + N_{arr}$ is the
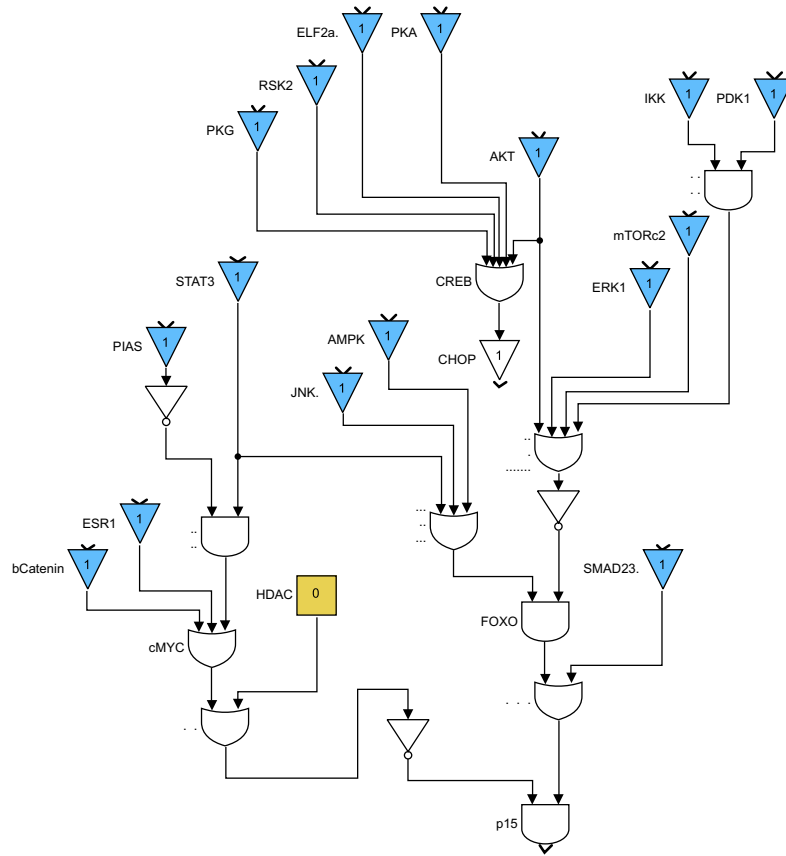
Figure 4.5: Cell proliferation pathways

total number of output factors. In both the Equations 3.5 and 4.6, the symbol $\sum$ stands for the average of the factors. The Convex-Sum metric as a whole measures the influence of a particular node on both cell death and cell cycle arrest.

Simulation Results

Each GBM cell line has different genetic mutations. We consider 9 GBM cell lines and their corresponding cellular mutations are given in Table 4.3. This information has been obtained using the GDSC database [20].

The set of input conditions should reflect that the stemness pathways are active in the cancer cells and the immune system has started to respond to the cancer. The stemness-related genes
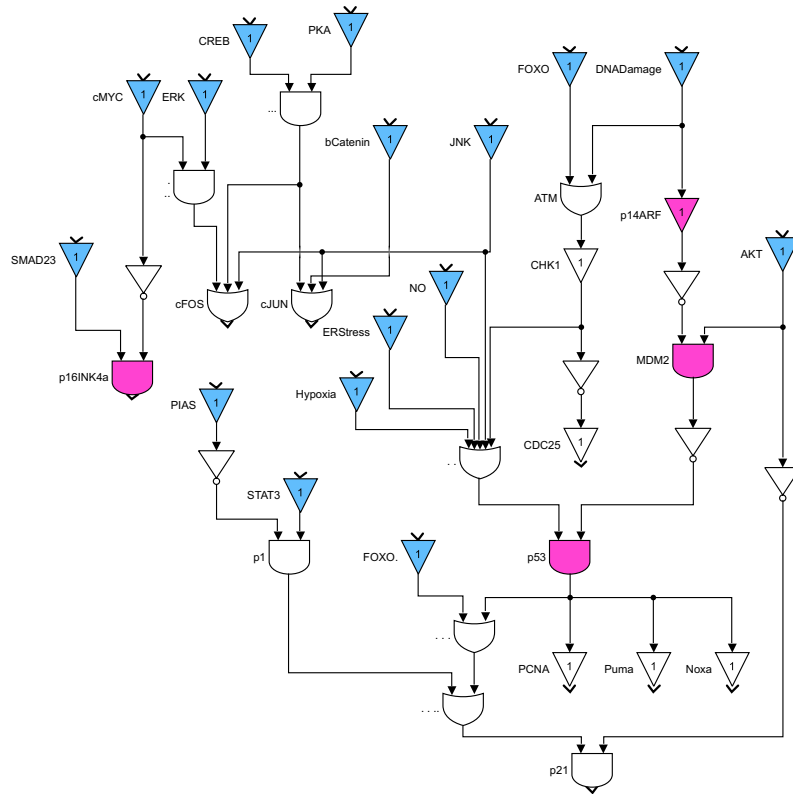
Figure 4.6: DNA damage and repair pathways

Table 4.3: GBM cell lines with different mutations

Cell Line Name	Genetic Mutations
42-MG-BA	p16INK4a, p14ARF, PDGFR, PTEN, p53
A172	p16INK4a, p14ARF, EGFR, p53
AM-38	p16INK4a, p14ARF, BRAF
CCF-STTG1	EGFR, MDM2, PTEN
LN-229	FasL, p16INK4a, p14ARF, EGFR,48
T98G	FasL, p16INK4a, p14ARF, p53
U-87-MG	FasL, p16INK4a, p14ARF, PTEN, NF1
YKG-1	p16INK4a, p14ARF, p53, PTEN, PI3K, NF1

Shh and Wnt are responsible to activate the stemness pathways as can be seen in Figure. 4.1. The immune system response is controlled by cytokines including IL17, TNF and TGFb as shown in Figures 4.2 and 4.7. For this purpose, the input vector for the simulations has been assigned
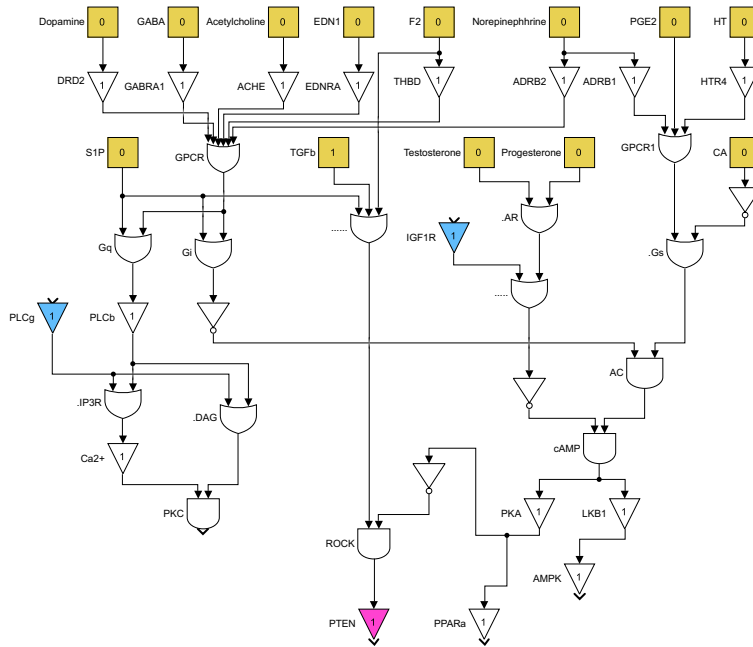
Figure 4.7: G-coupled protein and calcium signaling pathways
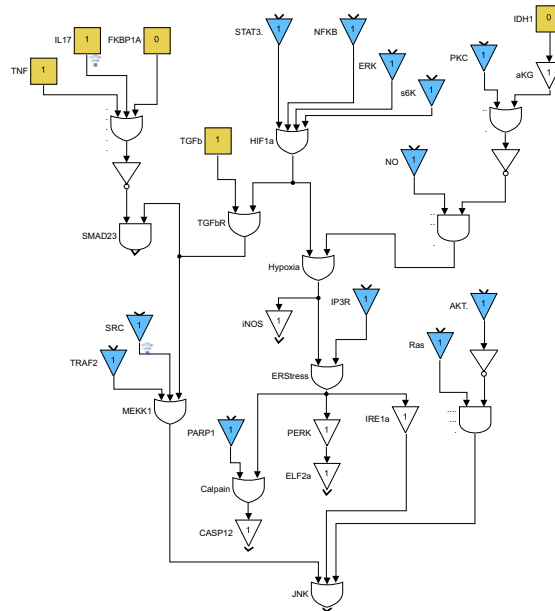
Figure 4.8: Hypoxia and endoplasmic reticulum stress pathways

the value $[1, 1, 0, 1, 1, 1, 0, 1, 0, 0, 0, 0, 0, 0, 0, 0, 0, 0, 0, 0, 0, 1]$; this implies that Shh, Wnt, IL17, Cytokine, TNF, TGFb and NF1 are all set to one and the other inputs are set to zero.

Prioritization of Genetic Targets for the GBM Cell line U-87 MG

For our first simulation, we choose one GBM cell line 'U-87 MG'. There are 5 faults in the cell line and the corresponding faults vector is shown in Eq. 4.8. All the faults in this fault vector are stuck-at-0 faults. We shall assign the value $[1, 1, 1, 1, 1]$ to the fault vector, which means that all the 5 faults are active and that FasL, p16INK4a, p14ARF, PTEN and NF1 are all down-regulated.

$$\text{Fault} = [\text{FasL}, \text{p16INK4a}, \text{p14ARF}, \text{PTEN}, \text{NF1}] \tag{4.8}$$

We will demonstrate the results of our ranking technique given the genetic profile of the cell line. Figure. 4.9 shows the results of prioritization for single genetic targets; the darker shade of purple implies greater priority of the target. For instance, NFKB and BCL-XL are two targets that have the same priority as each other, but have lower rank than p53. Similarly, in Figure. 4.10, the pairs of (fos, p53), (jun, p53) and (CDK4, p53) are the best pairs to target. In both the Figures 4.9 and 4.10, a red cell implies that the target should be inhibited and a green cell implies that a target should be expressed. We can use these results to find drugs that act on these genetic targets and have the desired action on those targets. For example, if we want to design a single target therapy with the best efficacy for a patient with genetic mutations similar to U-87 MG, we should look for a drug that activates p53. Using this functionality, we could move towards a personalized medicine
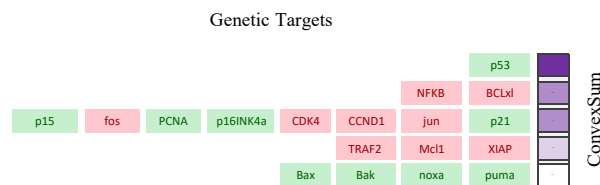
Figure 4.9: Prioritization of single targets for Glioblastoma therapy
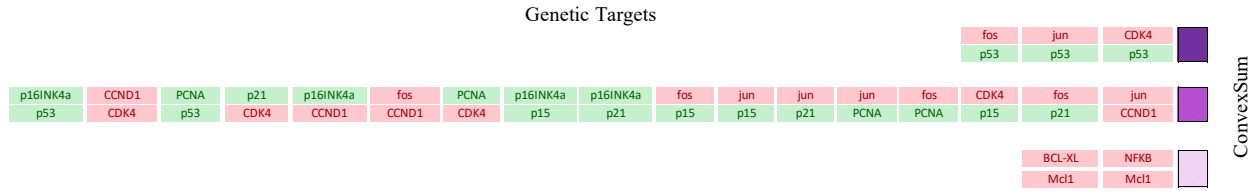
Figure 4.10: Prioritization of pairs of targets for Glioblastoma therapy

approach. The patient's genetic mutations could be fed into the algorithm as faults, and we could perform the prioritization task to identify the key intervention points specifically effective for that patient. We could use the prioritization results to design new drugs or drug therapies to treat GBM.

Drug Sensitivity for Anti-cancer and Non-cancer drugs

The second simulation is run to test drug sensitivity for each different GBM cell line. This functionality is similar to the one available in GDSC. We only included this functionality to plot the drug sensitivity for non-cancer drugs. The data for the drugs and their targets is from the GDSC database and DrugBank [20, 80]. Table. 4.4 shows the drug with its corresponding targets. Figure. 4.11 shows the drug sensitivity for anti-cancer drugs as predicted by the Boolean model; each row corresponds to a GBM cancer cell line and each column is a drug. Figure. 4.12 shows the drug sensitivity for non-cancer drugs as predicted by the Boolean model. In both Figures 4.11 and 4.12, a red cell implies that the drug does not work on that particular cell line and a green cell stands for a drug with a high efficacy. We can see that Aspirin seems to work on many GBM cell lines, but it fails to induce cell death or stop proliferation in AM-38 or LN-229. Yellow cells are the drugs that do not cause a significant change in the value of the Convex-Sum metric. Temozolomide, in Figure. 4.11, does not have much effect on any of the GBM cell lines; this might indicate that these cell lines have developed resistance to TMZ.

Increasing Sensitivity to Temozolomide

We ran a simulation for the cell line U-87 MG to test whether it is possible to reduce the resistance to TMZ. Figure. 4.13 shows that only the combination of Aspirin and TMZ is able to
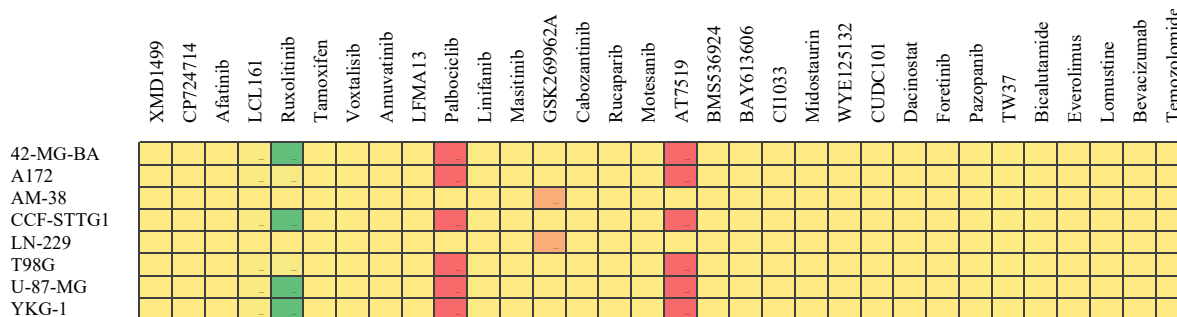
Figure 4.11: Drug sensitivity for anti-cancer drugs
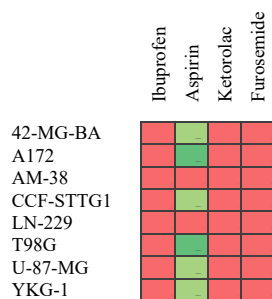
Figure 4.12: Drug sensitivity for non-cancer drugs

increase sensitivity of the cancer cells to TMZ. LC161 has only a slight effect on increasing the sensitivity to TMZ, but the rest of the drugs seem to be unable to have any effect. This tells us that while treating a patient with a genetic profile similar to U-87 MG, we might need to look at other two-drug or multi-drug therapies.

Best Two-drug Combinations for GBM Treatment

We can predict the best two-drug combination of anti-cancer and non-cancer drugs that can work for the U-87 MG GBM cell line. Figure. 4.14 shows only the top 35 two-drug combinations; the darker shade of green implies higher efficacy. For instance, the combination of LC-161 and Aspirin is yellowish green, which corresponds to a lower efficacy than the rest of the combinations shown in the figure. The best two combinations are Ruxolitinib + Palbociclib and Ruxolitinib +

EFFICACY	DRUG PAIR	
	Aspirin	Temozolomide
	LCL161	Temozolomide
	Ibuprofen	Temozolomide
	Ketorolac	Temozolomide
	Furosemide	Temozolomide
	XMD1499	Temozolomide
	CP724714	Temozolomide
	Afatinib	Temozolomide
	Tamoxifen	Temozolomide
	Voxtalisib	Temozolomide
	Amuvatinib	Temozolomide
	LFMA13	Temozolomide
	Linifanib	Temozolomide
	Masitinib	Temozolomide
	GSK269962A	Temozolomide
	Cabozantinib	Temozolomide
	Rucaparib	Temozolomide
	Motesanib	Temozolomide
	BMS536924	Temozolomide
	BAY613606	Temozolomide
	CI1033	Temozolomide
	Midostaurin	Temozolomide
	WYE125132	Temozolomide
	CUDC101	Temozolomide
	Dacinostat	Temozolomide
	Foretinib	Temozolomide
	Pazopanib	Temozolomide
	TW37	Temozolomide
	Bicalutamide	Temozolomide
	Everolimus	Temozolomide
	Lomustine	Temozolomide
	Bevacizumab	Temozolomide
	Temozolomide	Temozolomide
	Ruxolitinib	Temozolomide
	Palbociclib	Temozolomide
	AT7519	Temozolomide

Figure 4.13: Temozolomide in combination with one drug at a time.

AT7519; both these combinations have equal efficacy and perform 37% better than the next best combination. It is interesting to note that Aspirin features in the top 35 combinations, it is a non-cancer drug and not usually considered while designing drug therapies for GBM treatment. This functionality could be extended to test the combination of n number of drugs and then to find

EFFICACY	DRUG PAIR	
	Ruxolitinib	Palbociclib
	Ruxolitinib	AT7519
	XMD1499	Ruxolitinib
	Ruxolitinib	Tamoxifen
	Ruxolitinib	Aspirin
	GSK269962A	Aspirin
	CP724714	Ruxolitinib
	Afatinib	Ruxolitinib
	Ruxolitinib	Ruxolitinib
	Ruxolitinib	Voxtalisib
	Ruxolitinib	Amuvatinib
	Ruxolitinib	LFMA13
	Ruxolitinib	Linifanib
	Ruxolitinib	Masitinib
	Ruxolitinib	Cabozantinib
	Ruxolitinib	Rucaparib
	Ruxolitinib	Motesanib
	Ruxolitinib	BMS536924
	Ruxolitinib	BAY613606
	Ruxolitinib	CI1033
	Ruxolitinib	Midostaurin
	Ruxolitinib	WYE125132
	Ruxolitinib	CUDC101
	Ruxolitinib	Dacinostat
	Ruxolitinib	Foretinib
	Ruxolitinib	Pazopanib
	Ruxolitinib	TW37
	Ruxolitinib	Bicalutamide
	Ruxolitinib	Everolimus
	Ruxolitinib	Lomustine
	Ruxolitinib	Bevacizumab
	Ruxolitinib	Ibuprofen
	Ruxolitinib	Ketorolac
	Ruxolitinib	Furosemide
	LCL161	Aspirin

Figure 4.14: Top performing two drug combinations for Glioblastoma

the optimal drug combination (from the existing drugs available in the market) customized to the patient's genetic profile. It could also be used to predict the efficacies of multi-drug therapies that could potentially kill GBM cells or stop the spread of the cancer.

Table 4.4: Anti-cancer and non-cancer drugs with their targets

Number	Drug	Genetic Target
1	XMD1499	ALK, CDK4
2	CP724714	ERBB2
3	Afatinib	ERBB2, EGFR
4	LCL161	XIAP
5	Ruxolitinib	JAK1
6	Tamoxifen	ESR1
7	Voxtalisib	PI3K, MTOR
8	Amuvatinib	KIT, PDGFR, FLT3
9	LFMA13	BTK
10	Palbociclib	CDK4
11	Linifanib	VEGF, KDR, FLT3, FLT4, KIT
12	Masitinib	KIT, PDGFR
13	GSK269962A	ROCK
14	Cabozantinib	KDR, MET, KIT, FLT1, FLT3, FLT4
15	Rucaparib	PARP1
16	Motesanib	KDR, KIT, PDGFR
17	AT7519	CDK4
18	BMS536924	IGF1R
19	BAY613606	SYK
20	CI1033	EGFR, ERBB2
21	Midostaurin	PKC,FLT1
22	WYE125132	mTOR
23	CUDC101	HDAC1, EGFR, ERBB2
24	Dacinostat	HDAC1
25	Foretinib	MET, KDR, FLT4, PDGFR, FGF2, EGFR
26	Pazopanib	KIT, PDGFR
27	TW37	BCL2, BCL-XL, MCL1
28	Bicalutamide	AR
29	Everolimus	MTOR
30	Lomustine	IDH1, MGMT
31	Bevacizumab	FasL
32	Temozolomide	OG
33	Ibuprofen	THBD, Gp1BA, COX2, PPARa, PPARg, BCL2
34	Aspirin	EDNRA, ERK, NFKB, AMPK, RSK2, COX2, cMYC, p53, PCNA
35	Ketorolac	COX2
36	Furosemide	CA

5. CONCLUSIONS

We modeled the TRAIL resistant metastatic melanoma network using a Boolean network. The effects of Cryptotanshinone in combination with a few other drugs were studied. Simulations were run to study the effectiveness of Cryptotanshinone in increasing TRAIL sensitivity. The theoretically predicted efficacies seem to be borne out by the experimental results.

We modeled the induction of apoptosis by Cryptotanshinone in OS using a Boolean network. The effects of Cryptotanshinone in combination with other drugs were evaluated. The PI3K/mTOR pathway plays an important role in decreasing TRAIL sensitivity in OS. The results of the simulation indicate HIF1α as a key intervention point in inducing apoptosis in OS cell lines. Upon further biological investigation, we were able to make a strong case for CT as an effective STAT3 inhibitor and a valid candidate for OS therapy.

We modeled the biological pathways instrumental in glioblastoma and identified drug therapies that could prove to be effective for GBM treatment. We predicted a prioritization of genetic targets given the genetic profile of a patient. The Boolean model predicts that Aspirin, a non-cancer drug, could potentially reduce the resistance to Temozolomide in GBM patients; it could also be effective in combination with other chemotherapeutic drugs. Finally, we predicted two-drug therapies that could be more successful than the currently used treatment strategies.

REFERENCES

[1] R. S. Saraf, A. Datta, C. Sima, J. Hua, R. Lopes, and M. Bittner, "An in-silico study examining the induction of apoptosis by cryptotanshinone in metastatic melanoma cell lines," *BMC Cancer*, vol. 18, p. 855, 2018.

[2] A. Datta and E. R. Dougherty, *Introduction to Genomic Signal Processing with Control*. CRC Press, 2006.

[3] R. Layek, A. Datta, M. Bittner, and E. R. Dougherty, "Cancer therapy design based on pathway logic," *Bioinformatics*, vol. 27, no. 4, pp. 548—555, 2011.

[4] D. P. Cahill, K. W. Kinzler, B. Vogelstein, and C. Lengauer, "Genetic instability and darwinian selection in tumours," *Trends in Cell Biology*, vol. 9, no. 12, pp. M57–M60, 1999.

[5] M. Kanehisa and S. Goto, "Kegg: Kyoto encyclopedia of genes and genomes," *Nucleic Acids Research*, vol. 28, no. 1, p. 27–30, 2000.

[6] M. Kanehisa, M. Furumichi, M. Tanabe, Y. Sato, and K. Morishima, "Kegg: new perspectives on genomes, pathways, diseases and drugs," *Nucleic Acids Research*, vol. 45, no. 1, pp. D353—D361, 2016.

[7] M. Kanehisa, Y. Sato, M. Kawashima, M. Furumichi, and M. Tanabe, "Kegg: new perspectives on genomes, pathways, diseases and drugs," *Nucleic Acids Research*, vol. 44, no. 1, pp. D457—D462, 2016.

[8] P. S. Venkat, K. R. Narayanan, and A. Datta, "A bayesian network-based approach to selection of intervention points in the mitogen-activated protein kinase plant defense response pathway," *Journal of Computational Biology*, vol. 24, no. 4, 2017.

[9] O. A. Arshad and **A. Datta**, "Towards targeted combinatorial therapy design for the treatment of castration-resistant prostate cancer," *BMC Bioinformatics*, vol. 18 (Supp 4), p. 134, 2017.

[10] X.-P. Zhang, F. Liu, Z. Cheng, and W. Wang, "Cell fate decision mediated by p53 pulses," *PNAS*, vol. 106, pp. 12245–12250, 2009.

[11] S. Strano, S. Dell'Orso, S. Di Agostino, G. Fontemaggi, A. Sacchi, and G. Blandino, "Mutant p53: an oncogenic transcription factor," *Oncogene*, vol. 26, pp. 2212—-2219, 2007.

[12] J. Xu, J.-Y. Zhou, W.-Z. Wei, and G. S. Wu, "Activation of the akt survival pathway contributes to trail resistance in cancer cells," *PLOS one*, 2010.

[13] N. Corazza, D. Kassahn, S. Jakob, A. Badmann, and T. Brunner, "Trail-induced apoptosis: Between tumor therapy and immunopathology," *Annals of the New York Academy of Science*, vol. 1171, pp. 50—58, 2009.

[14] M. Abdelaleem, H. Ezzat, M. Osama, A. Megahed, W. Alaa, A. Gaber, A. Shafei, and A. Refaat, "Prospects for repurposing cns drugs for cancer treatment," *Oncology Reviews*, vol. 13, p. 411, 2019.

[15] B. Zagidullin, J. Aldahdooh, S. Zheng, W. Wang, Y. Wang, J. Saad, A. Malyutina, M. Jafari, Z. Tanoli, A. Pessia, and J. Tang, "Drugcomb: an integrative cancer drug combination data portal," *Nucleic Acids Research*, vol. 47, pp. 43–51, 2019.

[16] P. K. Sorgera and B. Schoeber, "An expanding role for cell biologists in drug discovery and pharmacology," *Molecular Biology of the Cell*, vol. 23, pp. 4162—-4164, 2012.

[17] M. A. Lindsay, "Target discovery," *Nature Reviews Drug Discovery*, vol. 2, pp. 831—838, 2018.

[18] N. Chang, S. H. Ahn, H. W. Lee, and D.-H. Nam, "The role of stat3 in glioblastoma progression through dual influences on tumor cells and the immune microenvironment.," *Molecular and Cellular Endocrinology*, vol. 451, pp. 53–65, 2017.

[19] F. M. Behan, F. Iorio, G. Picco, E. Gonçalves, C. M. Beaver, G. Migliardi, R. Santos, Y. Rao, F. Sassi, M. Pinnelli, R. Ansari, S. Harper, D. A. Jackson, R. McRae, R. Pooley, P. Wilkinson, D. van der Meer, D. Dow, C. Buser-Doepner, A. Bertotti, L. Trusolino, E. A. Stronach,

J. Saez-Rodriguez, K. Yusa, and M. J. Garnett, "Prioritization of cancer therapeutic targets using crispr–cas9 screens," *Nature*, vol. 568, pp. 511—516, 2019.

[20] W. Yang, J. Soares, P. Greninger, E. J. Edelman, H. Lightfoot, S. Forbes, N. Bindal1, D. Beare1, J. A. Smith, I. R. Thompson, S. Ramaswamy, P. A. Futreal, D. A. Haber, M. R. Stratton, C. Benes, U. McDermott, and M. J. Garnett, "Genomics of drug sensitivity in cancer (gdsc): a resource for therapeutic biomarker discovery in cancer cells.," *Nucleic Acids Research*, vol. 41, pp. 955–961, 2013.

[21] H. Liu, Y. Ma, S. M. Cole, C. Zander, K.-H. Chen, J. Karras, and R. M. Pope, "Serine phosphorylation of stat3 is essential for mcl-1 expression and macrophage survival," *Blood*, vol. 102, no. 1, pp. 344–352, 2003.

[22] D. E. Levy and C.-k. Lee, "What does stat3 do?," *Journal of CLinical Investigation*, vol. 109, no. 9, pp. 1143—-1148, 2002.

[23] V. N. Ivanov, M. A. Partridge, S. X. Huang, and T. K. Hei, "Suppression of the proinflammatory response of metastatic melanoma cells increases trail-induced apoptosis," *Journal of Cellular Biochemistry*, vol. 112, no. 2, pp. 463–475, 2011.

[24] G. P. Meares, R. Liu, Yudongand Rajbhandari, H. Qin, S. E. Nozell, J. A. Mobley, J. A. Corbett, and E. N. Benvenistea, "Perk-dependent activation of jak1 and stat3 contributes to endoplasmic reticulum stress-induced inflammation," *Molecular and Cellular Biology*, vol. 34, no. 20, pp. 3911—-3925, 2014.

[25] D. J. Gough, A. Corlett, K. Schlessinger, J. Wegrzyn, A. C. Larner, and D. E. Levy, "Mitochondrial stat3 supports ras-dependent oncogenic transformation," *Science*, vol. 324, pp. 1713–1716, 2009.

[26] R. Yang and M. Rincon, "Mitochondrial stat3, the need for design thinking," *International Journal of Biological Science*, vol. 12, no. 5, pp. 532–544, 2016.

[27] S.-A. Quast, K. Steinhorst, M. Plötz, and J. Eberle, "Sensitization of melanoma cells for death ligand trail is based on cell cycle arrest, ros production, and activation of proapoptotic bcl-2 proteins," *Journal of Investigative Dermatology*, vol. 135, pp. 2794—2804, 2015.

[28] H. Nakamura, A. Taguchi, K. Kawana, A. Kawata, M. Yoshida, A. Fujimoto, J. Ogishima, M. Sato, T. Inoue, H. Nishida, H. Furuya, K. Tomio, S. Eguchi, M. Mori-Uchino, A. Yamashita, K. Adachi, T. Arimoto, O. Wada-Hiraike, K. Oda, T. Nagamatsu, Y. Osuga, and T. Fujii, "Stat3 activity regulates sensitivity to tumor necrosis factor-related apoptosis-inducing ligand-induced apoptosis in cervical cancer cells.," *International Journal of Oncology*, vol. 49, no. 5, pp. 2155–2162, 2016.

[29] I. M. S. V., "Artesunate acts as fuel to fire in sensitizing hepg2 cells towards trail mediated apoptosis via stat3 inhibition and dr4 augmentation," *Biomedicine & Pharmacotherapy*, vol. 88, pp. 515–520, 2017.

[30] A. K.-W. Tse, K.-Y. Chow, H.-H. Cao, C.-Y. Cheng, H.-Y. Kwan, H. Yu, G.-Y. Zhu, Y.-C. Wu, W.-F. Fong, and Z.-L. Yu, "The herbal compound cryptotanshinone restores sensitivity in cancer cells that are resistant to the tumor necrosis factor-related apoptosis-inducing ligand," *Journal of Cellular Biochemistry*, vol. 288, no. 41, pp. 29923–29933, 2013.

[31] L. Lu, S. Zhang, C. Li, C. Zhou, D. Li, P. Liu, M. Huang, and X. Shen, "Cryptotanshinone inhibits human glioma cell proliferation in vitro and in vivo through shp-2-dependent inhibition of stat3 activation," *Cell Death & Disease*, vol. 8, p. 2767, 2017.

[32] Z. Chen, R. Zhu, C. Zheng, Jiayi Chen, C. Huang, J. Ma, C. Xu, W. Zhai, and J. Zheng, "Cryptotanshinone inhibits proliferation yet induces apoptosis by suppressing stat3 signals in renal cell carcinoma," *Oncotarget*, vol. 8, no. 30, pp. 50023—-50033, 2017.

[33] M. E. Hegi, "Mgmt gene silencing and benefit from temozolomide in glioblastoma," *The New England Journal of Medicine*, vol. 352, pp. 997–1003, 2005.

[34] J. Dul, L. M. Johnson, S. E. Jacobsen, and D. J. Patel, "Dna methylation pathways and their crosstalk with histone methylation," *Nature Reviews Molecular Cell Biology*, vol. 16,

pp. 519–532, 2015.

[35] X. D. Zhang, J. J. Wu, S. Gillespie, J. Borrow, and P. Hersey, "Cross resistance of melanoma to trail-induced apoptosis and chemotherapy," *Update on Cancer Therapeutics*, vol. 1, no. 4, pp. 435–441, 2006.

[36] M. J. Smyth, K. Takeda, Y. Hayakawa, J. J. Peschon, M. R. van den Brink, and H. Yagita, "Nature's trail—on a path to cancer immunotherapy," *Immunity*, vol. 18, no. 1, pp. 1–6, 2003.

[37] J. Eberle, "Bcl-2 proteins and trail resistance in melanoma," *In :TRAIL, Fas Ligand, TNF and TLR3 in Cancer. Resistance to Targeted Anti-Cancer Therapeutics*, vol. 12, 2017.

[38] M. S. Soengas and S. W. Lowe, "Apoptosis and melanoma chemoresistance," *Oncogene*, vol. 22, pp. 3138—3151, 2003.

[39] P. Hersey and X. D. Zhang, "How melanoma cells evade trail-induced apoptosis," *Nature Reviews Cancer*, vol. 1, pp. 142–150, 2001.

[40] L. W. Thomas, C. Lam, and S. W. Edwards, "Mcl-1; the molecular regulation of protein function," *FEBS Letters*, vol. 584, no. 14, pp. 2981—2989, 2010.

[41] C. Fleury, B. Mignotte, and J.-L. Vayssière, "Mitochondrial reactive oxygen species in cell death signaling," *Biochimie*, vol. 84, no. 2-3, pp. 131–141, 2002.

[42] S. W. G. Tait and D. R. Green, "Mitochondria and cell death: outer membrane permeabilization and beyond," *Molecular Cell Biology*, vol. 11, no. 9, pp. 621–632, 2010.

[43] M. C. Mendoza, E. E. Er, and J. Blenis, "The ras-erk and pi3k-mtor pathways:cross-talk and compensation," *Trends in Biochemical Sciences*, vol. 36, no. 6, pp. 320–328, 2012.

[44] D. Saleiro and L. C. Platanias, "Intersection of mtor and stat signaling in immunity," *Trends in Immunology*, vol. 36, no. 1, pp. 21–29, 2015.

[45] E. Flashner-Abramson, S. Klein, G. Mullin, E. Shoshan, R. Song, A. Shir, Y. Langut, M. Bar-Eli, H. Reuveni, and A. Levitzki, "Targeting melanoma with nt157 by blocking stat3 and igf1r signaling," *Oncogene*, vol. 35, pp. 2675—-2680, 2016.

[46] W. Chen, G. Lu, Yinand Chen, and S. Huang, "Cryptotanshinone has diverse effects on cell cycle events in melanoma cell lines with different metastatic capacity," *Cancer Chemotherapy and Pharmacology*, vol. 68, pp. 17–27, 2011.

[47] Y.-h. Wei, H.-x. Tang, Y.-d. Liao, S.-l. Fu, L.-q. Xu, G. Chen, C. Zhang, S. Ju, Z.-g. Liu, L.-k. You, L. Yu, and S. Zhou, "Effects of insulin-like growth factor 1 receptor and its inhibitor ag1024 on the progress of lung cancer," *Journal of Huazhong University of Science and Technology [Medical Sciences]*, vol. 35, no. 6, pp. 834–841, 2015.

[48] F. Chiarini, C. Grimaldi, F. Ricci, P. Tazzari, I. Iacobucci, G. Martinelli, P. Pagliaro, J. Mc-Cubrey, S. Amadori, and A. M. Martelli, "Temsirolimus, an allosteric mtorc1 inhibitor, is synergistic with clofarabine in aml and aml leukemia initiating cells," *Blood*, vol. 118, p. 2596, 2011.

[49] P. Yue, F. Lopez-Tapia, D. Paladino, Y. Li, C.-H. Chen, A. T. Namanja, T. Hilliard, Y. Chen, M. A. Tius, and J. Turkson, "Hydroxamic acid and benzoic acid–based stat3 inhibitors suppress human glioma and breast cancer phenotypes in vitro and in vivo," *Cancer Research*, vol. 76, no. 3, pp. 652–663, 2016.

[50] S. Jamil, S. Mojtabavi, P. Hojabrpour, S. Cheah, and V. Duronio, "An essential role for mcl-1 in atr-mediated chk1 phosphorylation," *Molecular Biology of the Cell*, vol. 19, no. 8, pp. 3212—3220, 2008.

[51] J. Hua, C. Sima, M. Cypert, G. Gooden, S. Shack, L. Alla, E. Smith, J. M. Trent, E. R. Dougherty, and M. L. Bittner, "Tracking transcriptional activities with high-content epifluorescent imaging," *Journal of Biomedical Optics*, vol. 17, p. 046008, 2012.

[52] M. Szewczyk, R. Lechowski, and K. Zabielska, "What do we know about canine osteosarcoma treatment? review.," *Veterinary Research Communications*, vol. 39, pp. 61–67, 2015.

[53] G. Ottaviani and N. Jaffe, "Pediatric and adolescent osteosarcoma," *Cancer Treatment and Research*, vol. 152, pp. 15–32, 2009.

[54] J. J. Morrowa and C. Khannab, "Osteosarcoma genetics and epigenetics: Emerging biology and candidate therapies," *Critical Reviews in Oncogenesis*, vol. 20, pp. 173–197, 2015.

[55] A. Nguyen, V. Nguyen, D. Pham, M. Mravic, M. A. Scott, and A. W. James, "Novel signaling pathways in osteosarcoma," *International Journal of Orthopaedics*, vol. 1, pp. 73–84, 2014.

[56] P. Angulo, G. Kaushik, D. Subramaniam, P. Dandawate, K. Neville, K. Chastain, and S. Anant, "Natural compounds targeting major cell signaling pathways: a novel paradigm for osteosarcoma therapy," *Journal of Hematology & Oncology*, vol. 10, pp. 4649–4653, 2017.

[57] M. Paoloni, S. Davis, S. Lana, S. Withrow, L. Sangiorgi, P. Picci, S. Hewitt, T. Triche, P. Meltzer, and C. Khanna, "Canine tumor cross-species genomics uncovers targets linked to osteosarcoma progression," *BMC Genomics*, vol. 10, p. 625, 2009.

[58] C. Vogel, A. Chan, B. Gril, S.-B. Kim, J. Kurebayashi, L. Liu, Y.-S. Lu, and H. Moon, "Management of erbb2-positive breast cancer: insights from preclinical and clinical studies with lapatinib." *Japanese Journal of Clinical Oncology*, vol. 40, pp. 999–1013, 2010.

[59] S. L. Fossey, A. T. Liao, J. K. McCleese, M. D. Bear, J. Lin, P.-K. Li, W. C. Kisseberth, and C. A. London, "Characterization of stat3 activation and expression in canine and human osteosarcoma," *BMC Cancer*, vol. 9, p. 81, 2009.

[60] C. Khanna, T. M. Fan, R. Gorlick, L. J. Helman, E. S. Kleinerman, P. C. Adamson, P. J. Houghton, W. D. Tap, D. R. Welch, P. S. Steeg, G. Merlino, P. H. Sorensen, D. G. Kirsch, K. A. Janeway, B. Weigel, R. L. Randall, P. Meltzer, S. J. Withrow, M. Paoloni, R. N. Kaplan, B. A. Teicher, N. L. Seibel, A. Uren, S. R. Patel, J. Trent, S. A. Savage, L. Mirabello, D. Reinke, D. A. Barkauskas, M. Krailo, M. A. Smith, and M. Bernstein, "Toward a drug development path that targets metastatic progression in osteosarcoma." *Clinical Cancer Research*, vol. 20, pp. 4200–4209, 2014.

[61] M. S. Isakoff, S. S. Bielack, P. Meltzer, and R. Gorlick, "Osteosarcoma : Treatment and a collaborative pathway to success," *Journal Of Clinical Oncology*, vol. 33, pp. 3029–3035, 2015.

[62] T.-a. Matsui, Y. Sowa, T. Yoshida, H. Murata, M. Horinaka, M. Wakada, R. Nakanishi, T. Sakabe, T. Kubo, and T. Sakai, "Sulforaphane enhances trail-induced apoptosis through the induction of dr5 expression in human osteosarcoma cells," *Carcinogenesis*, vol. 27, pp. 1768–1777, 2006.

[63] G. Picarda, F. Lamoureux, L. Geffroy, P. Delepine, T. Montier, K. Laud, F. Tirode, O. Delattre, D. Heymann, and F. Rédini, "Preclininal evidence that use of trail in ewing's sarcoma and ostosarcoma therapy inibits tumor growth, prevents osteolysis and increases animal survival," *Clinical Cancer Research*, 2010.

[64] B. Tu, J. Zhu, S. Liu, L. Wang, Q. Fan, Y. Hao, C. Fan, and T.-T. Tang, "Mesenchymal stem cells promote osteosarcoma cell survival and drug resistance through activation of stat3," *Oncotarget*, vol. 7, pp. 48296–48308, 2016.

[65] Y. Zhang, S. B. Cabarcas, J. Zheng, L. Sun, L. A. Mathews, X. Zhang, H. Lin, and W. Farrar, "Cryptotanshinone targets tumor-initiating cells through down-regulation of stemness genes expression," *Oncology Letters*, vol. 11, pp. 3803–3812, 2016.

[66] J.-H. Yen, H. S. Huang, C. J. Chuang, and S.-T. Huang, "Activation of dynamin-related protein 1 - dependent mitochondria fragmentation and suppression of osteosarcoma by cryptotanshinone," *Journal of Experimental and Clinical Cancer Research*, vol. 38, no. 2, 2019.

[67] T. Rampias, R. Favicchio, J. Stebbing, and G. Giamas, "Targeting tumor stroma crosstalk: the example of the nt157 inhibitor," *Oncogene*, vol. 35, pp. 2562–2564, 2016.

[68] M. K. Rasmussen, L. Iversen, C. Johansen, J. Finnemann, L. S. Olsen, K. Kragballe, and B. Gesser, "Il-8 and p53 are inversely regulated through jnk, p38 and nf-kappab p65 in hepg2 cells during an inflammatory response," *Inflammation Research*, vol. 57, no. 7, pp. 329–339, 2008.

[69] J. H. Lin, P. Walter, and B. T. Yen, "Endoplasmic reticulum stress in disease pathogenesis," *Annual Review of Pathology: Mechanisms of Disease*, vol. 3, pp. 399–425, 2008.

[70] Y.-G. Ren, K. W. Wagner, D. A. Knee, P. Aza-Blanc, M. Nasoff, and Q. L. Deveraux, "Differential regulation of the trail death receptors dr4 and dr5 by the signal recognition particle," *Molecular Biology of the Cell*, vol. 15, no. 11, pp. 5064—-5074, 2004.

[71] Y. Lu, G.-F. Guan, J. Chen, B. Hu, C. Sun, Q. Ma, Y.-H. Wen, X.-C. Qiu, and Y. Zhou, "Aberrant cxcr4 and β-catenin expression in osteosarcoma correlates with patient survival," *Oncology Letters*, vol. 10, no. 4, pp. 2123—-2129, 2015.

[72] R. M. Locklin, E. Federici, B. Espina, P. A. Hulley, R. G. G. Russell, and C. M. Edwards, "Selective targeting of death receptor 5 circumvents resistance of mg-63 osteosarcoma cells to trail-induced apoptosis," *Molecular Cancer Therapeutics*, vol. 6, no. 1, pp. 3219–3228, 2007.

[73] R. Stupp, W. P. Mason, M. J. van den Bent, M. Weller, B. Fisher, M. J. B. Taphoorn, K. Belanger, A. A. Brandes, C. Marosi, U. Bogdahn, J. Curschmann, R. C. Janzer, S. K. Ludwin, T. Gorlia, A. Allgeier, D. Lacombe, J. G. Cairncross, E. Eisenhauer, R. O. Mirimanoff, European Organisation for Research and Treatment of Cancer Brain Tumor and Radiotherapy Groups, and National Cancer Institute of Canada Clinical Trials Group, "Radiotherapy plus concomitant and adjuvant temozolomide for glioblastoma," *The New England Journal of Medicine*, vol. 352, pp. 987–996, Mar. 2005.

[74] R. Stupp, S. Taillibert, A. Kanner, W. Read, D. Steinberg, B. Lhermitte, S. Toms, A. Idbaih, M. S. Ahluwalia, K. Fink, F. Di Meco, F. Lieberman, J.-J. Zhu, G. Stragliotto, D. Tran, S. Brem, A. Hottinger, E. D. Kirson, G. Lavy-Shahaf, U. Weinberg, C.-Y. Kim, S.-H. Paek, G. Nicholas, J. Bruna, H. Hirte, M. Weller, Y. Palti, M. E. Hegi, and Z. Ram, "Effect of Tumor-Treating Fields Plus Maintenance Temozolomide vs Maintenance Temozolomide Alone on Survival in Patients With Glioblastoma: A Randomized Clinical Trial," *JAMA*, vol. 318, no. 23, pp. 2306–2316, 2017.

[75] C. Y. Lee, "Strategies of temozolomide in future glioblastoma treatment," *OncoTargets and therapy*, vol. 10, pp. 265–270, Jan. 2017.

[76] E. Ozdemir-Kaynak, A. A. Qutub, and O. Yesil-Celiktas, "Advances in Glioblastoma Multiforme Treatment: New Models for Nanoparticle Therapy," *Frontiers in Physiology*, vol. 9, Mar. 2018.

[77] S. Y. Lee, "Temozolomide resistance in glioblastoma multiforme," *Genes and Diseases*, vol. 3, no. 3, pp. 198–210, 2016.

[78] H. Yan, "Idh1 and idh2 mutations in gliomas," *The New England Journal of Medicine*, vol. 360, pp. 765–773, 2009.

[79] A. Cohen, S. Holmen, and H. Colman, "Idh1 and idh2 mutations in gliomas," *Current Neurology and Neuroscience Reports*, vol. 13, p. 345, 2013.

[80] G. A. S. S. H. M. S. P. C. Z. W. J. Wishart DS, Knox C, "Drugbank: a comprehensive resource for in silico drug discovery and exploration," *Nucleic Acids Research*, vol. 34, pp. 668–672, 2006.